

Screening of a Phosphite–Phosphoramidite Ligand Library for Palladium-Catalysed Asymmetric Allylic Substitution Reactions: The Origin of Enantioselectivity

Oscar Pàmies* and Montserrat Diéguez*[a]

Abstract: We have designed a new library of readily available, highly modular phosphite-phosphoramidite ligands for asymmetric allylic substitution reactions. They are easily prepared in one step from commercially available chiral 1,2-amino alcohols. The introduction of a phosphoramidite moiety into the ligand design is highly advantageous

for the product outcome. This ligand library affords high reaction rates (TOFs of up to 800 mol(mol h)⁻¹) and enantioselectivities (*ees* of up to 99%) and,

Keywords: allylic substitution • asymmetric catalysis • enantioselectivity • palladium • pi ligands

at the same time, contains a broad range of disubstituted hindered and unhindered substrate types. NMR study of the Pd- π -allyl intermediates provide a deeper understanding of the effect of the ligand parameters on the origin of enantioselectivity.

Introduction

The development of methods for enantioselective carbon–carbon and carbon–heteroatom bond formation is one of the key issues in organic synthesis. A versatile method for forming these bonds is palladium-catalysed asymmetric allylic substitution with nucleophiles.^[1] Numerous chiral ligands, mainly phosphorus- and nitrogen-containing ligands, which have either C₂ or C₁ symmetry, have provided high enantiomeric excesses.^[1] Most of the chiral ligands developed for asymmetric allylic substitution reactions are mixed bidentate donor ligands (such as P–N, P–S and S–N).^[1,2] The efficiency of this type of hard–soft heterodonor ligand has mainly been attributed to the different electronic effects of the donor atoms. However, to a lesser extent, homodonor ligands (e.g., Trost’s diphosphines) have also demonstrated their potential usefulness in this process largely because of the chiral discrimination induced by the C₂ or C₁ symmetry of the ligand backbone.^[1] However, one disadvantage of these homo- and hetero-donor ligand systems is that they

are often synthesised either from expensive chiral sources or in tedious synthetic steps. Another common disadvantage of the most successful ligand families developed so far for this process is that they usually have low reaction rates and a high substrate specificity (Figure 1, i.e., high *ee* values are obtained in disubstituted linear hindered substrates and low *ees* are obtained in unhindered substrates, or vice versa).^[1]

Therefore research into more versatile and reactive ligand systems synthesised in a few steps from simple starting materials is of great importance. In view of this, a group of less electron-rich phosphorus homodonor compounds (diphosphite ligands) have been shown to be able to overcome these limitations and to be useful in this process.^[3] However, considerable dependence on the backbone has been observed. Thus, enantioselectivities were excellent with 1,3-diphosphites (*ees* of up to 99%), whereas the 1,2-diphosphites were less enantioselective (*ees* of up to 80%) (Figure 2).^[3a]

Because of the high enantioselectivity induced by mixed bidentate donor ligands in this process,^[1] the decision was made to design a new family of ligands based on 1,2-diphosphite ligands (Figure 2b) in which one of the phosphite groups is replaced by a phosphoramidite moiety (Figure 2c). This new phosphite-phosphoramidite ligand design therefore offers the opportunity of electronic differentiation whilst maintaining a similar spatial disposition around the metal centre. Moreover, the high activities obtained with diphosphite ligands^[4] are expected to be maintained in these phosphite-phosphoramidite ligands because the phosphoramidite moiety is also a good π -acceptor group.^[5] We therefore

[a] Dr. O. Pàmies, Dr. M. Diéguez
Departament de Química Física i Inorgànica
Universitat Rovira i Virgili
C/Marcel·lí Domingo s/n, 43007 Tarragona (Spain)
Fax: (+34)977559563
E-mail: oscar.pamies@urv.cat
montserrat.dieguez@urv.cat

Supporting information for this article is available on the WWW under <http://www.chemeurj.org/> or from the author.

	PHOX ligands	Trost's ligands	Evans' ligands
	100% Yield (1 h) 99% ee	9% Yield (24 h) 52% ee	100% Yield (24 h) 98% ee
	99% Yield (1 h) 85% ee	92% Yield (24 h) 91% ee	87% Yield (24 h) 65% ee
	Yield not reported 72% ee	86% Yield (6 h) 96% ee	100% Yield (24 h) 90% ee
	99% Yield (18h) 47% regio; 84% ee	-	-

Figure 1. Summary of the best results obtained with several linear and cyclic substrates with three of the most representative ligand families developed for palladium-catalysed allylic substitution reactions (reactions were usually carried out with 2–4 mol % of palladium).

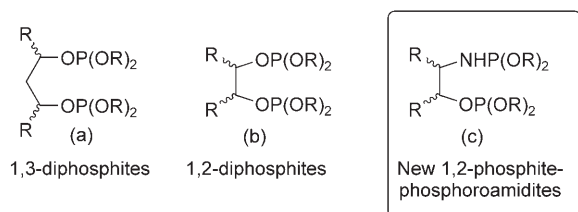


Figure 2. Diphosphite and phosphite-phosphoramidite structures.

report herein the design of a library of 60 potential chiral phosphite-phosphoramidite ligands **1–10a–f** (Figure 3) for use in palladium-catalysed allylic substitution reactions.^[6] We also discuss the synthesis and characterisation of the Pd- π -allyl intermediates in order to provide a greater insight into the origin of the enantioselectivity. The library was synthesised and screened by using a series of parallel reactors, each of which was equipped with 12 different positions. These new phosphite-phosphoramidite ligands **1–10a–f** also have the advantage of a flexible ligand scaffold so that the substituents/configurations of the amino alcohol backbone (C-1 and C-2), the amino group and the biaryl moieties (**a–f**) can be easily tuned to explore how they affect the catalytic performance. As a result, highly enantioselective and active palladium-catalysed allylic substitution reactions of several substrates with different steric properties have been carried out.^[1] Another important advantage of these phosphite-phosphoramidite ligands is that they can be readily synthesised in one step from commercially available chiral 1,2-amino alcohols (see below). Therefore this ligand design will overcome the drawbacks of high substrate specificity, low activity and tedious synthesis so characteristic of other ligand families successfully developed for palladium-catalysed allylic substitution reactions.^[1]

Despite the advantages of phosphite-phosphoramidite ligands, they have been little used in asymmetric catalysis.^[7] To the best of our knowledge only one family of phosphite-

phosphoramidite ligands successfully has been used in allylic substitution reactions.^[5b] More research is therefore needed to study the possibilities offered by phosphite-phosphoramidites as a new class of ligand for this process.

Results and Discussion

Ligand synthesis: The synthesis of the new phosphite-phosphoramidite ligands **1–10a–f** is straightforward (Scheme 1). They are synthesised very efficiently in one step from the corresponding commercially available cheap 1,2-amino alco-

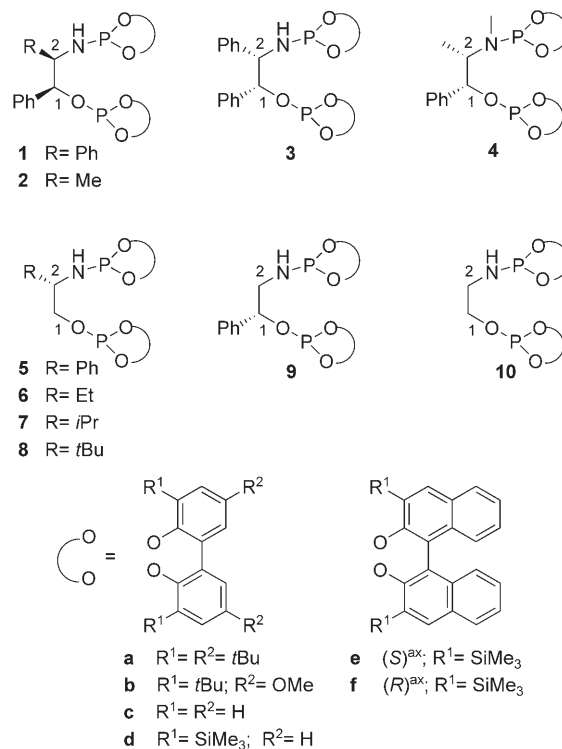
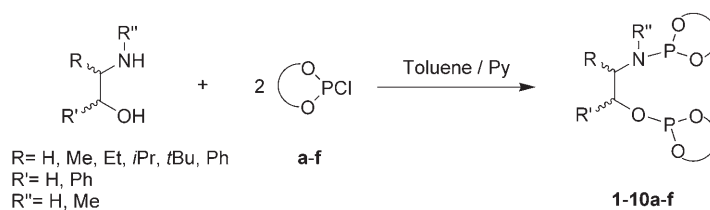
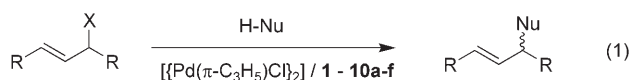


Figure 3. Phosphite-phosphoramidite ligand library **1–10a–f**.



hols by reaction with two equivalents of the desired in situ formed phosphorochloridite (**a–f**) in the presence of a base. All the ligands were stable during purification on neutral alumina under an atmosphere of argon and isolated in moderate-to-good yields as white solids. They are stable at room temperature and very stable to hydrolysis. The elemental analyses were in agreement with the structure assigned. The ^1H and ^{13}C NMR spectra are in accord with those expected for these C_1 ligands. Two singlets for each compound were observed in the ^{31}P NMR spectra. Rapid ring inversions (atropoisomerisation) of the biphenyl-phosphorus moieties (**a–d**) occurred on the NMR timescale as the expected diastereoisomers were not detected by low-temperature ^{31}P NMR spectroscopy.^[8]

Allylic substitution of disubstituted linear substrates: In this section, we report on the use of the chiral phosphite-phosphoramidite ligand library (**1–10a–f**) in the palladium-catalysed allylic substitution [Eq. (1)] of three disubstituted linear substrates with different steric properties: *rac*-1,3-diphenyl-3-acetoxyprop-1-ene (**S1**) (widely used as a model substrate), ethyl *rac*-(*E*)-2,5-dimethylhept-4-en-3-yl carbonate (**S2**) and *rac*-1,3-dimethyl-3-acetoxyprop-1-ene (**S3**). Two nucleophiles were tested. In all cases, the catalysts were generated in situ from the π -allyl-palladium chloride dimer $[\{\text{PdCl}(\eta^3\text{-C}_3\text{H}_5)_2\}]_2$ and the corresponding ligand.



- | | |
|--|--|
| S1 R = Ph; X = OAc | 11 R = Ph; H-Nu = H-CH(COOMe) ₂ |
| S2 R = <i>i</i> Pr; X = OCO ₂ Et | 12 R = Ph; H-Nu = H-NHCH ₂ Ph |
| S3 R = Me; X = OAc | 13 R = <i>i</i> Pr; H-Nu = H-CH(COOMe) ₂ |
| | 14 R = Me; H-Nu = H-CH(COOMe) ₂ |

Allylic substitution of *rac*-1,3-diphenyl-3-acetoxyprop-1-ene (S1**) using dimethyl malonate and benzylamine as nucleophiles:** For an initial evaluation of this new type of ligand in the palladium-catalysed asymmetric substitution reactions, we chose the allylic substitution of **S1** [Eq. (1), R = Ph; X = OAc] and used dimethyl malonate and benzylamine as the nucleophiles. As these reactions were carried out with a variety of ligands carrying different donor groups, the efficacy of different ligand systems can be directly compared.^[1]

In the first set of experiments, we determined the optimal reaction conditions by conducting a series of experiments in which the solvent and the ligand-to-palladium ratio were varied. We first studied the effect of four solvents (tetrahydrofuran (THF), toluene, dimethylformamide (DMF) and dichloromethane (DCM)) with six ligands (**1a–5a** and **9a**). Figure 4 shows the results obtained when dimethyl malonate was used as the nucleophile (trends were similar in the allylic amination of **S1**, see the Supporting Information). The results show that the efficiency of the process strongly depended on the nature of the solvent. The activities and enantioselectivities were best with dichloromethane as solvent

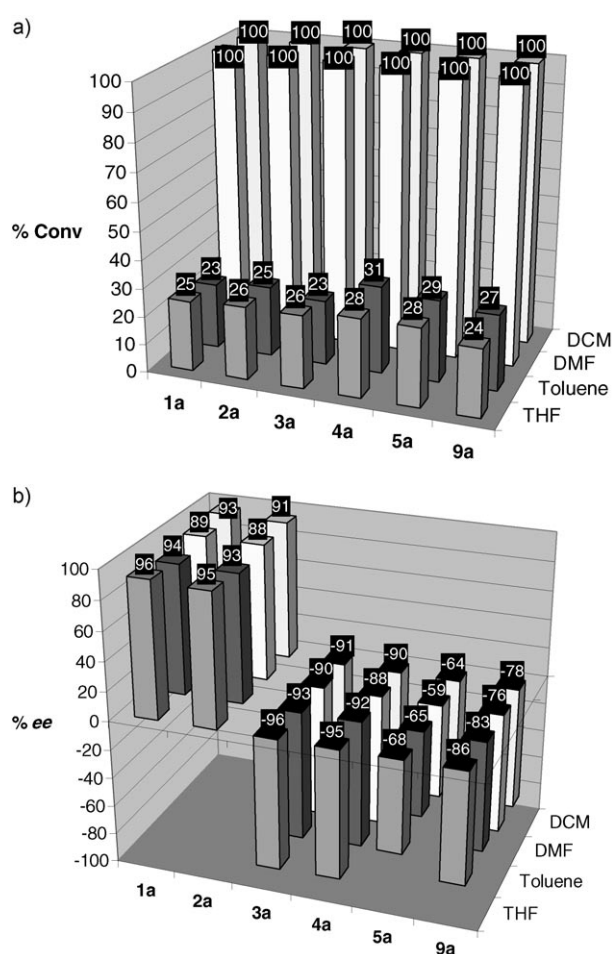


Figure 4. Results of the catalytic allylic alkylation of **S1** obtained by using ligands **1–5a** and **9a** in four solvents at room temperature. a) Conversions after 15 min. b) Enantioselectivities of product **11**. Positive numbers refer to the formation in excess of the *R* isomer.

(Figure 5). We then studied the effect of varying the ligand-to-palladium ratio. The conversions and enantioselectivities obtained when dichloromethane and ligands **1a–5a** and **9a**

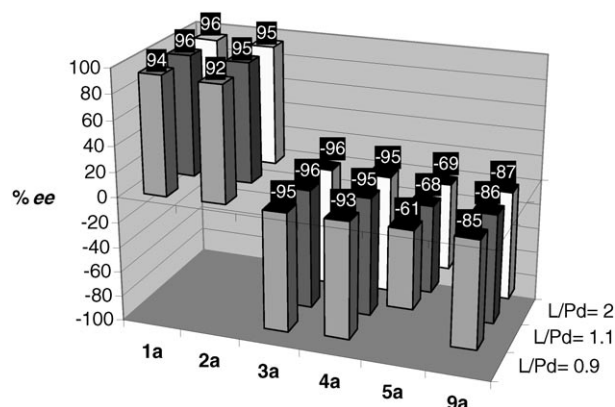


Figure 5. Enantioselectivities of product **11** obtained by using ligands **1–5a** and **9a** at different ligand-to-palladium ratios in dichloromethane at room temperature. Positive numbers refer to the formation in excess of the *R* isomer. In all cases full conversion was obtained after 15 min.

were used are shown in Figure 5 (similar trends were observed for the other solvents). The results show that an excess of ligand is not needed for activities and enantioselectivities to be high.

For comparison purposes, the rest of the ligands were tested under conditions that provided optimum enantioselectivities and reaction rates (i.e., a ligand-to-palladium ratio of 1.1 and dichloromethane as solvent). Table 1 shows

Table 1. Palladium-catalysed allylic substitution of **S1** using the phosphite-phosphoramidite ligand library **1–10a–f**.^[a]

Entry	Ligand	H–Nu=H–CH(COOMe) ₂		H–Nu=H–NHCH ₂ Ph	
		Conv. [%] (min) ^[b]	ee [%] ^[c]	Conv. [%] (h) ^[b]	ee [%] ^[c]
1	1a	100 (15)	96 (<i>R</i>)	100 (12)	97 (<i>S</i>)
2	1b	100 (25)	92 (<i>R</i>)	100 (24)	90 (<i>S</i>)
3	1c	41 (15)	6 (<i>R</i>)	79 (24)	2 (<i>S</i>)
4	1d	100 (15)	71 (<i>R</i>)	100 (12)	78 (<i>S</i>)
5	1e	100 (15)	94 (<i>R</i>)	100 (12)	93 (<i>S</i>)
6	1f	100 (15)	94 (<i>S</i>)	100 (12)	94 (<i>R</i>)
7	2a	100 (15)	95 (<i>R</i>)	100 (12)	94 (<i>S</i>)
8	3a	100 (15)	96 (<i>S</i>)	100 (12)	97 (<i>R</i>)
9	3d	100 (15)	71 (<i>S</i>)	100 (12)	76 (<i>R</i>)
10	3f	100 (15)	94 (<i>S</i>)	100 (12)	93 (<i>R</i>)
11	4a	100 (15)	95 (<i>S</i>)	100 (12)	96 (<i>R</i>)
12	5a	100 (15)	68 (<i>S</i>)	100 (12)	71 (<i>R</i>)
13	6a	100 (15)	31 (<i>S</i>)	100 (12)	28 (<i>R</i>)
14	7a	100 (15)	14 (<i>R</i>)	100 (12)	9 (<i>S</i>)
15	8a	100 (15)	70 (<i>R</i>)	100 (12)	68 (<i>S</i>)
16	9a	100 (15)	86 (<i>S</i>)	100 (12)	85 (<i>R</i>)
17	10f	81 (15)	89 (<i>S</i>)	100 (24)	88 (<i>R</i>)
18 ^[d]	1a	100 (120)	99 (<i>R</i>)	–	–
19 ^[e]	1a	100 (65)	96 (<i>R</i>)	–	–

[a] All reactions were run at 23 °C with 0.5 mol% [[PdCl(η³-C₃H₅)₂]₂], 1.1 mol% ligand and dichloromethane as solvent. [b] The reaction time is shown in parentheses. [c] Enantiomeric excess. The absolute configuration is given in parentheses. [d] *T* = 5 °C. [e] **S1**/Pd = 500.

the results when dimethyl malonate and benzylamine were used as the nucleophiles. They indicate that catalytic performance (activities and enantioselectivities) is highly affected by the substituents and the axial chirality of the biaryl moieties and the substituents in the amino alcohol backbone. In general, activities (TOFs of up to 800 mol **S1** (mol Pd h)^{−1}) and enantioselectivities (*ees* of up to 99%) were high. Although, as expected, the activities for the amination process were lower than for the alkylation reaction of **S1**, they were higher than those obtained with other successful ligands.^[1] The stereoselectivity of the amination reaction was the same as that of the alkylation reaction, although the Cahn–Ingold–Prelog (CIP) descriptor was inverted due to the change in priority of the groups.

The effect of the biphenyl substituents was investigated with ligands **1a–d** (Table 1, entries 1–4). It was observed that these moieties affect both the activity and the enantioselectivity of the reaction. Bulky substituents in the *ortho* and *para* positions of the biphenyl moieties are needed for high enantioselectivity. Therefore ligand **1a** with bulky *tert*-butyl groups in both the *ortho* and *para* positions of the biphenyl moieties provided the highest enantioselectivity

(Table 1, entry 1). In terms of activity, this is mainly affected by the substituents in the *ortho* positions of the biphenyl moieties. Therefore ligands **1a**, **1b** and **1d**, with bulky substituents in the *ortho* positions of the biphenyl moieties, provided much higher activities than ligand **1c**, which has small hydrogen atoms in these positions (Table 1, entries 1, 2 and 4 vs. 3). The substituents in the *para* positions also play a small but crucial role. Thus, whereas the activities were excellent with ligands **1a** and **1d**, the activity decreased slightly for ligand **1b** which contains methoxy groups in the *para* positions (Table 1, entries 1 and 4 versus 2). The activity and enantioselectivity are therefore at their highest with ligand **1a**, which contains *tert*-butyl groups in both the *ortho* and *para* positions of the biphenyl moieties. To further investigate how the enantioselectivity is influenced by the groups attached to the biaryl moiety, ligands **1e** and **1f**, which contain different enantiomerically pure bulky trimethylsilylbiphenyl moieties, were also tested (Table 1, entries 5 and 6). The results indicate that the sense of the enantioselectivity is governed by the configuration of these biaryl moieties. Therefore both enantiomers of the substitution products **11** and **12** can be accessed in high enantioselectivity simply by changing the absolute configuration of the biaryl moieties. Accordingly, ligand **1e**, with the binaphthyl groups in the *S* configuration, gave (*R*)-**11** and (*S*)-**12** products, whereas ligand **1f**, with the binaphthyl groups in the *R* configuration, gave (*S*)-**11** and (*R*)-**12** products.

The effects of the substituents and the configuration of the amino alcohol backbone (carbon atoms C-1 and C-2) and the amino group were studied with ligands **1–9a**, **1f**, **3f** and **10f** (Table 1, entries 1, 6–8 and 10–17). We found that the nature of the amino alcohol backbone affected the enantioselectivity whereas the substituent on the amino group hardly affected it at all. No effect on the activity was observed. Therefore it is necessary for substituents to be in both positions of the amino alcohol backbone (carbon atoms C-1 and C-2) if the enantioselectivities are to be high. Accordingly, ligands **1–3a**, substituted at both the C-1 and C-2 atoms of the amino alcohol backbone, provided higher enantioselectivities than ligands **5–9a** which are substituted at only one carbon atom (Table 1, entries 1, 7 and 8 versus 12–16). For monosubstituted ligands **5–9**, we also found that a substituent in the C-1 position of the amino alcohol backbone is more effective at transferring chiral information to the allylic substitution products **11** and **12** than a substituent in the C-2 position. Therefore ligand **9a**, substituted with a phenyl group at the C-1 atom of the amino alcohol backbone, provides better enantioselectivity than the related ligand **5a** substituted at C-2 (Table 1, entries 12 versus 16). Finally, the results obtained when ligand **1a** and **3a** were used, which only differ in the C-1 and C-2 configurations of the amino alcohol backbone, indicate that the sense of enantioselectivity is also governed by the configuration of these stereogenic centres. Therefore both enantiomers of products **11** and **12** can also be accessed in high enantioselectivities simply by changing the absolute configuration of the amino alcohol unit (Table 1, entries 1 versus 8).

If we compare the results obtained by using ligands **1a,d** and **3a,d** with those obtained by using **1e,f** and **3f**, we can also conclude that the configuration of the atropoisomerically fluxional biphenyl moieties in ligands **1-4a-d** is controlled by the configuration of the amino alcohol ligand backbone.^[9] Nevertheless, the efficiency of transferring chiral information from the amino alcohol backbone to the biphenyl moieties depends on the type of substituents in the ligand backbone (**1-10**) and the substituents in the biaryl groups (**a-d**).

The enantioselectivity was further improved (*ees* of up to 99%) with ligand **1a** by lowering the reaction temperature to 5 °C (Table 1, entry 18). The reaction was also performed at a low catalyst concentration (**S1**/Pd=500) with ligand **1a**. Both the enantioselectivity (96% *ee* (*R*)) and the activity (TOFs of up to 800 mol **S1**(mol Pdh)⁻¹) remained high (Table 1, entry 19).

In summary, for enantioselectivities to be high, the substituents in the amino alcohol backbone need to be correctly combined and enantiopure bulky biaryl moieties must be present. These enantiopure biaryl moieties can either be introduced by using chiral binaphthyl groups (ligands **1e** and **1f**) or generated in situ by using *ortho*- and *para*-substituted bulky atropoisomeric biphenyl moieties with the appropriate substitution/configuration in the amino alcohol ligand backbone (ligands **1-4a**). For high activities, bulky substituents need to be located in the *ortho* positions of the biaryl moieties. Accordingly, the best results (*ees* of up to 99% and TOFs of up to 800 mol **S1**(mol Pdh)⁻¹) were obtained with ligands **1-4a**, **1e,f** and **3f** which contain the optimal combination of substituents/configurations of the biaryl moieties and the amino alcohol backbone. Interestingly, both enantiomers of the substitution products **11** and **12** can be accessed in high enantioselectivity simply by changing either the absolute configuration of the biaryl moieties or the absolute configuration of the amino alcohol unit. These results clearly show the efficiency of using modular scaffolds in the ligand design. In addition, when these excellent results are compared with the activities and enantioselectivities obtained with the corresponding Pd-1,2-phosphinite-amino-phosphine (*ees* of up to 60%)^[10] and Pd-1,2-diphosphite (*ees* of up to 80%)^[3a] catalytic systems, we can conclude that the introduction of a phosphoramidite moiety into ligands **1-10a-f** has been extremely advantageous. These results are among the best that have been reported.^[1]

Allylic alkylation of ethyl *rac*-(*E*)-2,6-dimethylhept-4-en-3-yl carbonate (S2**):** We also screened the phosphite-phosphoramidite ligand library **1-10a-f** in the allylic alkylation process of **S2** using dimethyl malonate as the nucleophile [Eq. (1), R = *i*Pr, X = OCO₂Et]. This substrate is more sterically demanding than substrate **S1**.^[1] The most noteworthy results are shown in Table 2. In general they follow the same trends as observed for the allylic alkylation of **S1**, which is not unexpected because the reactions proceed through a similar mechanism.^[1] Again, the catalyst precursor containing the phosphite-phosphoramidite ligands **1-4a**, **1e** and **1f** provided the best enantioselectivities (Table 2, en-

Table 2. Selected results for the palladium-catalysed allylic alkylation of **S2** using the ligand library **1-10a-f**.^[a]

Entry	Ligand	Conv. [%] (h) ^[b]	<i>ee</i> [%] ^[c]
1	1a	100 (18)	> 95 (<i>S</i>)
2	1b	78 (18)	93 (<i>S</i>)
3	1c	64 (18)	3 (<i>S</i>)
4	1d	100 (18)	79 (<i>S</i>)
5	1e	100 (18)	> 95 (<i>S</i>)
6	1f	100 (18)	> 95 (<i>R</i>)
7	2a	100 (18)	93 (<i>S</i>)
8	3a	100 (18)	95 (<i>R</i>)
9	4a	100 (18)	95 (<i>R</i>)
10	5a	100 (18)	72 (<i>R</i>)
11	6a	100 (18)	31 (<i>R</i>)
12	7a	100 (18)	19 (<i>S</i>)
13	8a	100 (18)	73 (<i>S</i>)
14	9a	100 (18)	89 (<i>R</i>)
15	10f	82 (18)	91 (<i>R</i>)

[a] All reactions were run at 23 °C with 0.5 mol% [[PdCl(η³-C₃H₅)₂], 1.1 mol% ligand and CH₂Cl₂ as solvent. [b] The reaction time in hours is given in parentheses. [c] Enantiomeric excess. The absolute configuration is given in parentheses.

tries 1, 5–9). As expected the activities were lower than in the alkylation reaction of **S1**.^[1] The stereoselectivity of the alkylation of **S2** was the same as that obtained in the alkylation of **S1** although the CIP descriptor was inverted because the priority of the groups had been changed.

Allylic alkylation of *rac*-1,3-dimethyl-3-acetoxyprop-1-ene (S3**) using dimethyl malonate as the nucleophile:** We also evaluated the phosphite-phosphoramidite ligand library **1-10a-f** in the allylic alkylation of the linear substrate **S3** [Eq. (1), R = Me, X = OAc]. This substrate is less sterically demanding than substrates **S1** and **S2**. The enantioselectivity was more difficult to control in the reactions with **S3** than with hindered substrates such as **S1** and **S2**. If the *ees* are to be high, the ligand must create a small chiral pocket (the chiral cavity in which the allyl is embedded) around the metal centre, mainly because of the presence of less sterically demanding *syn*-methyl substituents.^[1] Therefore few catalytic systems have provided high enantioselectivities.^[11]

The preliminary investigations carried out to optimise the solvent and ligand-to-palladium ratio revealed a different trend regarding the solvent effect compared with those observed with the previously tested substrates **S1** and **S2**. The selectivities and activities were best when THF was used and the ligand-to-palladium ratio was 1.1 (Table 3, entries 1–6).

The results obtained by using the phosphite-phosphoramidite ligand library **1-10a-f** under the optimised conditions are summarised in Table 3 (entries 4 and 7–23). In general, the activities and enantioselectivities were also high (*ees* of up to 85%) in the alkylation of **S3**. The activities followed the same trends as those observed in the alkylation of substrates **S1** and **S2** and were mainly affected by the substituents in the biaryl groups. The highest reaction rates were obtained with ligands containing bulky substituents in the

Table 3. Selected results for the palladium-catalysed allylic alkylation of **S3** using the ligand library **1–10a–f**.^[a]

Entry	Solvent	Ligand	Conv. [%] (min) ^[b]	ee [%] ^[c]
1	CH ₂ Cl ₂	1a	100 (20)	74 (S)
2	DMF	1a	100 (20)	73 (S)
3	toluene	1a	100 (20)	72 (S)
4	THF	1a	100 (20)	78 (S)
5 ^[d]	THF	1a	100 (20)	78 (S)
6 ^[e]	THF	1a	100 (20)	77 (S)
7	THF	1b	100 (30)	70 (S)
8	THF	1c	32 (30)	5 (S)
9	THF	1d	100 (20)	72 (S)
10	THF	1e	100 (20)	82 (R)
11	THF	1f	100 (20)	82 (S)
12	THF	2a	100 (20)	45 (S)
13	THF	3a	100 (20)	77 (R)
14	THF	4a	100 (20)	37 (R)
15	THF	5a	100 (20)	42 (R)
16	THF	6a	100 (20)	24 (R)
17	THF	7a	100 (20)	18 (R)
18	THF	8a	100 (20)	5 (S)
19	THF	9a	100 (20)	55 (S)
20	THF	10f	68 (30)	80 (S)
21 ^[f]	THF	1a	24 (120)	82 (S)
22 ^[f]	THF	1e	18 (120)	85 (R)
23 ^[f]	THF	1f	16 (120)	85 (S)

[a] All reactions were run at 23 °C with 0.5 mol % $[(\text{PdCl}(\eta^3\text{-C}_3\text{H}_5)_2)]_2$ and 1.1 mol % ligand. [b] The reaction time in minutes is given in parentheses. [c] Enantiomeric excess. The absolute configuration is given in parentheses. [d] **1a**/Pd=0.9. [e] **1a**/Pd=2. [f] $T = -5^\circ\text{C}$.

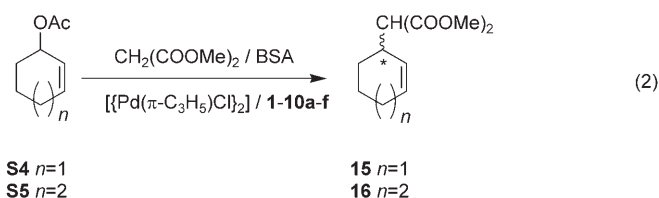
ortho positions of the biaryl moieties (TOFs of up to >300 mol **S3** (mol Pd h)⁻¹).

Again, the enantioselectivities were significantly affected by the substituents and the axial chirality of the biaryl moieties and the substituents on the amino alcohol backbone. However, the effect of these parameters was different to the effect observed in the alkylation of **S1** and **S2**. Thus, although the effect of the substituents/configurations of the biaryl moieties on enantioselectivity is similar to the effect observed in the alkylation of **S1** and **S2**, the effects of the substituents on the amino alcohol ligand backbone (C-1 and C-2) and on the amino group are different. Therefore, unlike the alkylation of **S1** and **S2**, the presence of a methyl substituent on either the amino group (ligand **4a**, Table 3, entry 13 versus 14) or the stereogenic carbon atom C-2 in the ligand backbone (ligand **2a**, Table 3, entry 4 versus 12) has a negative effect on the enantioselectivity. Also, ligand **10f**, which has a simple unsubstituted ethanolamine backbone, provides an enantioselectivity that is similar to that of ligand **1f** which has a 1,2-diphenylethanolamine backbone (Table 3, entries 11 versus 20). Again, both enantiomers of the alkylation product **14** can be accessed with high enantioselectivity simply by changing either the absolute configuration of the biaryl moieties or the absolute configuration of the amino alcohol unit. The best enantioselectivities (ees of up to 85%) were therefore obtained for ligands **1a,e,f**, **3a** and **10f** which have bulky substituents in the *ortho* and *para* positions of the biaryl moieties and the appropriate combination of substituents in the amino alcohol backbone. These results, which clearly show the efficiency of using highly

modular scaffolds in the ligand design, are amongst the best reported for this type of unhindered substrate.^[11] Again, the presence of a phosphoramidite moiety in the ligand design has been extremely advantageous in terms of the activity and enantioselectivity of the reaction.

Allylic alkylation of cyclic substrates: As for the unhindered substrate **S3**, the enantioselectivity of reactions involving cyclic substrates is difficult to control, mainly because of the presence of less steric *anti* substituents. These *anti* substituents are thought to play a crucial role in the enantioselectivity observed with cyclic substrates in the corresponding Pd-allyl intermediate.^[1]

We can also reveal that the chiral phosphite-phosphoramidite ligand library **1–10a–f** used above in the palladium-catalysed allylic substitution of linear substrates (**S1–S3**) can be used with cyclic substrates (ees of up to 95%). In this case, two cyclic substrates were tested [Eq. (2)]: *rac*-3-acetoxycyclohexene (**S4**) (which is widely used as a model substrate) and *rac*-3-acetoxycycloheptene (**S5**).



We initially studied the allylic alkylation of *rac*-3-acetoxycyclohexene (**S4**) by using ligands **1–10a–f**. Preliminary investigations into the solvent effect and the ligand-to-palladium ratio showed the same trends as those observed with the unhindered linear substrate **S3**. The trade-off between enantioselectivities and reaction rates was therefore optimum with tetrahydrofuran and a ligand-to-palladium ratio of 1.1 (Table 4, entries 1–6).

The results obtained by using the phosphite-phosphoramidite ligand library **1–10a–f** under the optimised conditions are summarised in Table 4 (entries 4 and 7–21). In general the activities and enantioselectivities of the allylic alkylation reactions were also high (ees of up to 81%) with **S4**. The activities were mainly affected by the biaryl groups. Bulky *tert*-butyl groups in the *ortho* positions of the biphenyl moieties are needed for high activities (TOFs of up to >200 mol **S4** (mol Pd h)⁻¹). Therefore ligands **1–9a,b**, which have bulky *tert*-butyl groups in the *ortho* positions of the biphenyl moieties, provide higher activities than ligands **1–9c–f**, which either have small hydrogen atoms (**c**) or bulky trimethylsilyl substituents (**d–f**) in these positions (Table 4, entries 4, 7, 12–19 versus 8–11). This trend contrasts those observed in the allylic substitution of disubstituted linear substrates **S1–S3**. The enantioselectivities were similar to those observed in the alkylation of unhindered disubstituted linear substrate **S3**. Therefore the best enantioselectivities (ees of up to 81%) were obtained for ligands **1a,e,f**, **3a** and **10f** (Table 4,

Table 4. Selected results for the palladium-catalysed allylic alkylation of cyclic substrates **S4** and **S5** using the ligand library **1–10a–f**.^[a]

Entry	Solvent	Ligand	Substrate	Conv. [%] (min) ^[b]	ee [%] ^[c]
1	CH ₂ Cl ₂	1a	S4	100 (15)	65 (<i>R</i>)
2	DMF	1a	S4	100 (15)	60 (<i>R</i>)
3	toluene	1a	S4	50 (30)	63 (<i>R</i>)
4	THF	1a	S4	100 (30)	71 (<i>R</i>)
5 ^[d]	THF	1a	S4	100 (30)	70 (<i>R</i>)
6 ^[e]	THF	1a	S4	100 (30)	71 (<i>R</i>)
7	THF	1b	S4	100 (30)	55 (<i>R</i>)
8	THF	1c	S4	9 (30)	0
9	THF	1d	S4	45 (30)	59 (<i>R</i>)
10	THF	1e	S4	18 (30)	70 (<i>S</i>)
11	THF	1f	S4	13 (30)	69 (<i>R</i>)
12	THF	2a	S4	100 (30)	55 (<i>R</i>)
13	THF	3a	S4	100 (30)	71 (<i>S</i>)
14	THF	4a	S4	100 (30)	30 (<i>S</i>)
15	THF	5a	S4	100 (30)	25 (<i>S</i>)
16	THF	6a	S4	100 (30)	21 (<i>S</i>)
17	THF	7a	S4	100 (30)	16 (<i>R</i>)
18	THF	8a	S4	100 (30)	5 (<i>S</i>)
19	THF	9a	S4	100 (30)	42 (<i>R</i>)
20	THF	10f	S4	24 (60)	74 (<i>R</i>)
21 ^[f]	THF	10f	S4	15 (360)	81 (<i>R</i>)
22	THF	1a	S5	39 (120)	92 (<i>R</i>)
23	THF	10f	S5	14 (120)	95 (<i>R</i>)

[a] All reactions were run at 23 °C with 0.5 mol % [[PdCl(η³-C₃H₅)₂]] and 1.1 mol % ligand. [b] Reaction time in minutes is given in parentheses. [c] Enantiomeric excess. The absolute configuration is given in parentheses. [d] **1a**/Pd=0.9. [e] **1a**/Pd=2. [f] T=0 °C.

entries 4, 10, 11, 13, 20 and 21). Again, both enantiomers of the alkylation product **15** can be easily accessed in high enantioselectivity by simply changing the absolute configuration of either the biaryl moiety or the amino alcohol unit.

This phosphite-phosphoramidite ligand library **1–10a–f** was also effective (*ees* of up to 95 %) in the allylic alkylation of the seven-membered ring substrate **S5** (Table 4, entries 22 and 23).

In summary, the results obtained with cyclic substrates are amongst the best reported so far.^[11a,c,d,12]

Allylic substitution of monosubstituted linear substrates:

Encouraged by the excellent results obtained for several disubstituted linear and cyclic substrates, we examined the regio- and stereoselective allylic alkylation of 1-(1-naphthyl)-allyl acetate (**S6**) and 1-(1-naphthyl)-3-acetoxyprop-1-ene (**S7**) with dimethyl malonate [Eq. (3)]. For these substrates, not only does the enantioselectivity of the process need to be controlled, the regioselectivity is also a problem because a mixture of regioisomers may be obtained. Most palladium

catalysts developed to date favour the formation of achiral linear product **18** rather than the desired branched isomer **17**.^[13] Therefore the development of highly regio- and enantioselective palladium catalysts is still a challenge.^[11c,14]

The results obtained with the phosphite-phosphoramidite ligand library **1–10a–f** are summarised in Table 5. In general good enantioselectivities (*ees* of up to 85 %) and moderate-to-good regioselectivities (up to 65 %) in favour of the branched product **17** were obtained under unoptimised reaction conditions. The results indicate that the regioselectivity of the reaction is mainly affected by the biaryl moieties. Therefore the best regioselectivities were obtained with ligands **1e,f** and **10f** (regioselectivities of up to 65 %) which contain bulky disubstituted

ortho-trimethylsilyl binaphthyl moieties (Table 5, entries 5, 6 and 15). In contrast, the enantioselectivity was mainly affected by both the biaryl moieties and the amino alcohol backbone. However, they do not affect the enantioselectivity in the same way as in the alkylation of disubstituted linear and cyclic substrates **S1–S5**. Therefore the best enantioselectivities were obtained by using ligand **4a** (*ees* of up to 85 %) which has a 1,2-diphenylethanolamine backbone and a methyl substituent on the amino group (Table 5, entry 9).

Origin of enantioselectivity: A Study of the Pd-π-allyl intermediates:

To provide further insight into how ligand parameters affect the catalytic performance, we studied the Pd-π-allyl compounds **19–25**, [Pd(π-allyl)(L)]BF₄ (L = phosphite-phosphoramidite ligands), as these are the key intermediates in the allylic substitution reactions studied.^[1] These ionic palladium complexes, which contain 1,3-diphenyl- and 1,3-dimethylallyl groups, were prepared by using the methodology previously described (Scheme 2) from the corresponding

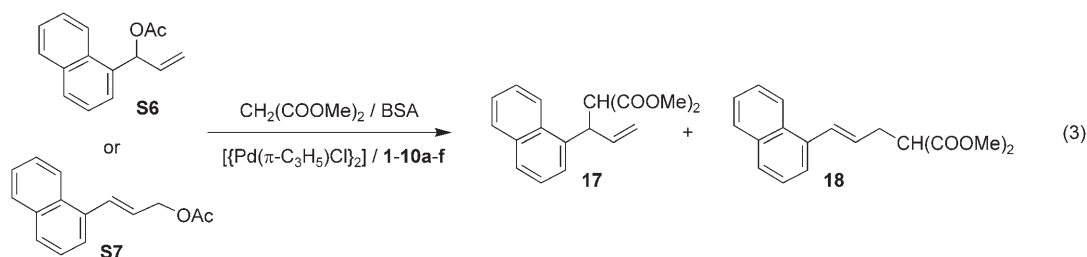


Table 5. Selected results for the palladium-catalysed allylic alkylation of monosubstituted substrates **S6** and **S7** using the ligand library **1–10 a–f** under standard conditions.^[a]

Entry	Ligand	Substrate	Conv. [%] ^[b] (min)	17/18 ^[c]	<i>ee</i> [%] ^[d]
1	1a	S6	100 (120)	30:70	68 (<i>R</i>)
2	1b	S6	100 (120)	35:65	25 (<i>R</i>)
3	1c	S6	100 (120)	25:75	38 (<i>S</i>)
4	1d	S6	100 (120)	45:55	16 (<i>R</i>)
5	1e	S6	100 (120)	65:35	50 (<i>S</i>)
6	1f	S6	100 (120)	65:35	47 (<i>R</i>)
7	2a	S6	100 (120)	30:70	79 (<i>R</i>)
8	3a	S6	100 (120)	30:70	71 (<i>S</i>)
9	4a	S6	100 (120)	30:70	85 (<i>S</i>)
10	5a	S6	100 (120)	25:75	49 (<i>S</i>)
11	6a	S6	100 (120)	30:70	57 (<i>S</i>)
12	7a	S6	100 (120)	25:75	35 (<i>S</i>)
13	8a	S6	100 (120)	20:80	13 (<i>R</i>)
14	9a	S6	100 (120)	45:55	54 (<i>S</i>)
15	10 f	S6	100 (120)	60:40	56 (<i>R</i>)
16	4a	S7	100 (120)	30:70	84 (<i>S</i>)

[a] All reactions were run at 23 °C with 1 mol % $[\text{PdCl}(\eta^3\text{-C}_3\text{H}_5)]_2$, 1.1 mol % ligand and dichloromethane as solvent. [b] The reaction time in minutes is given in parentheses. [c] Percentage of branched (**17**) and linear (**18**) isomers. [d] Enantiomeric excess. The absolute configuration is given in parentheses.

Scheme 2. Preparation of Pd- π -allyl complexes **19–25**.

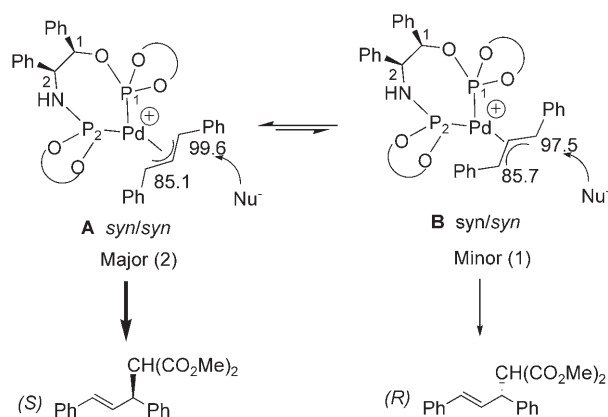
Pd-allyl dimer and the appropriate ligand in the presence of silver tetrafluoroborate.^[15] The complexes were characterised by elemental analysis and ¹H, ¹³C and ³¹P NMR spectroscopy. The spectral assignments (see the Experimental Section) were based on information from ¹H–¹H, ³¹P–¹H and ¹³C–¹H correlation measurements in combination with ¹H–¹H NOESY experiments. Unfortunately, it was not possible to obtain any crystals of sufficient quality to perform X-ray diffraction measurements.

Palladium-1,3-diphenylallyl complexes: When the phosphite-phosphoramidite ligand library **1–10 a–f** was used in the allylic substitution of disubstituted hindered substrates **S1** and **S2**, the results indicated that for the enantioselectivity to be high, a correct combination of the substitution/configuration of the biaryl moieties and the amino alcohol backbone needed to be present: 1) enantiopure binaphthyl moieties or *ortho*- and *para*-substituted biphenyl moieties are required if the enantioselectivity is to be high, 2) ligands must be substituted in both positions (C-1 and C-2) of the amino alcohol backbone if the enantioselectivity is to be high and 3) ligands substituted in the C-1 position of the amino alcohol backbone are more effective than ligands that are only substituted in the C-2 position. To understand this catalytic behaviour we decided to study the Pd- π -allyl

complexes **19–23** which contain ligands **3a**, **3d**, **3f**, **6a** and **9a**, respectively.

With complexes $[\text{Pd}(\eta^3\text{-1,3-diphenylallyl})(\mathbf{3a})]\text{BF}_4$ (**19**), $[\text{Pd}(\eta^3\text{-1,3-diphenylallyl})(\mathbf{3d})]\text{BF}_4$ (**20**) and $[\text{Pd}(\eta^3\text{-1,3-diphenylallyl})(\mathbf{3f})]\text{BF}_4$ (**21**), we studied the effect of the configuration/substitution of the biaryl moieties on the catalytic performance. These complexes maintain the same configuration/substitution in the amino alcohol backbone of the ligands, but differ in the configuration and the substituents on the biaryl moieties. The catalytic systems Pd/**3a** and Pd/**3f**, which contain substituents in both the *ortho* and *para* positions of the biphenyl moieties and enantiopure binaphthyl moieties, respectively, provided high enantioselectivities (*ees* of up to 96 %), but the catalytic system Pd/**3d**, which has no substituents in the *para* positions of the biphenyl group, was less enantioselective (*ees* of up to 71 %) (Table 1, entries 8–10). On the other hand, with complexes $[\text{Pd}(\eta^3\text{-1,3-diphenylallyl})(\mathbf{6a})]\text{BF}_4$ (**22**) and $[\text{Pd}(\eta^3\text{-1,3-diphenylallyl})(\mathbf{9a})]\text{BF}_4$ (**23**), the effect of the amino alcohol backbone on catalytic activity was studied. These catalytic systems, containing monosubstituted ligands **6a** and **9a**, are differentiated by the position of the substituent in the amino alcohol backbone. The Pd/**6a** system (Table 1, entry 13), which is only substituted at C-2 of the amino alcohol backbone, provides lower enantioselectivities than the palladium/disubstituted **3a**, **3d** and **3f** catalytic systems (Table 1, entries 8–10) and Pd/**9a** with the ligand substituted only at C-1 (Table 1, entry 16).

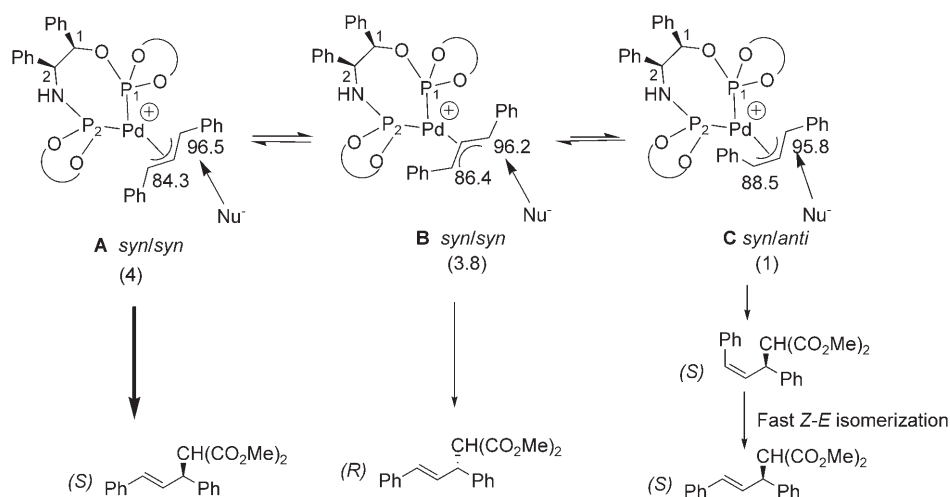
The NMR study of Pd-allyl intermediate **19**, which contains ligand **3a**, revealed a mixture of two isomers in a 2:1 ratio (see the Experimental Section). No changes were observed down to –80 °C. Both isomers were unambiguously assigned by NOE experiments to the two *syn/syn endo* and *exo* isomers (Scheme 3). The equilibrium between the diastereoisomers forms by the so-called apparent π -allyl rotation which has been shown to occur by dissociation of one of the coordinated atoms of the bidentate ligand which allows the ligand to rotate.^[16] For both isomers, the ¹³C NMR chemical shifts indicate that the more electrophilic allyl carbon terminus is *trans* to the phosphoramidite moiety. Assuming that the nucleophilic attack takes place at the more electrophilic carbon terminus and on the basis of the observed stereochemical outcome of the reaction, 96 % (*S*) for product **11** and the fact that the enantiomeric excess of the alkylation product **11** is higher than the diastereoisomeric excesses of the palladium intermediates, the **A** isomer must react faster than the **B** isomer. To prove this, the reac-



Scheme 3. Diastereoisomeric Pd-allyl intermediates for the reaction of **S1** with ligand **3a**. The relative amounts of each isomer are given in parentheses. The chemical shifts [ppm] of the allylic terminal carbon atoms are shown.

tivity of the palladium intermediates with sodium malonate at a low temperature was also studied by in situ NMR spectroscopy (Figure 6). The results show that the major isomer **A** reacts around 15 times faster than isomer **B**. Taking into account the relative reaction rates and the abundance of both isomers the calculated *ee* should be 94% (*S*), which matches the value obtained experimentally.^[17] Therefore it can be concluded that nucleophilic attack takes place at the allyl terminus *trans* to the phosphoramidite moiety of the major palladium intermediate **A**. This is also consistent with the fact that for both isomers, the most electrophilic allylic terminal carbon atom is the one *trans* to the phosphoramidite in the major **A** isomer.

In contrast to complex **19**, the NMR study of Pd-allyl intermediate **20**, which contains ligand **3d**, revealed a mixture of three isomers in a ratio 4:3.8:1 (see the Experimental Section, Scheme 4). The major isomers (**A** and **B**) were assigned by NOE experiments to the two *syn/syn* *endo* and *exo* isomers, whereas the minor isomer (**C**) was attributed to the *syn/anti* isomer (Scheme 4). For the **B** isomer, the VT-³¹P NMR experiments indicated that the phosphorus atom next to C-1 (P-1, assigned by ³¹P-¹H HMBC correlation experiments) showed fluxional behaviour and was frozen out at -20°C. A study of the models indicated that the absence of *para* substituents on the biphenyl groups in ligand **3d** compared with ligand **3a** favours the atropisomerism of the biphenyl moieties in isomer **B**. This atropisomerism causes a change in the configuration of the biphenyl



Scheme 4. Diastereoisomeric Pd-allyl intermediates for the reaction of **S1** with ligand **3d**. The relative amounts of each isomer are given in parentheses. The chemical shifts [ppm] of the allylic terminal carbon atoms are shown.

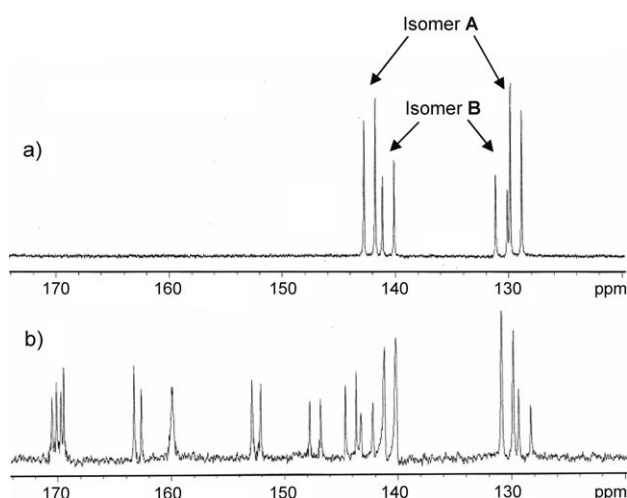


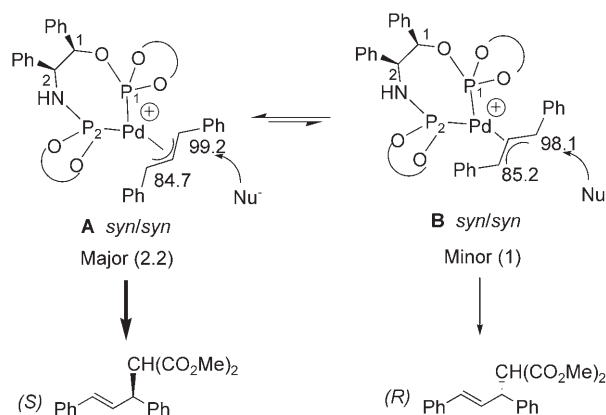
Figure 6. ³¹P{¹H} NMR spectra of [Pd(η^3 -1,3-diphenylallyl)(**3a**)]BF₄ (**19**) in CD₂Cl₂ at -60°C a) before and b) after the addition of sodium malonate.

moiety located at P-1 that produces an increase in the steric repulsion between one of the phenyl substituents of **S1** and one of the biphenyl moieties. The formation of the *syn/anti* isomers **C** minimises this new steric repulsion. Therefore the open Pd-C bond belongs to the most electrophilic carbon atom which bears the substituents that experience the biggest steric hindrance with the biaryl phosphite fragment P-1. As for complex **19**, note that, for all isomers, the more electrophilic allyl carbon terminus is *trans* to the phosphoramidite moiety and that isomer **A** reacts faster than the other isomers. Assuming that nucleophilic attack takes place at the most electrophilic carbon atom, attack at the *syn/syn* isomer **A** and at the *syn/anti* isomer **C** will lead to the formation of (*S*)-**11**, whereas attack on the *syn/syn* isomer **B** will lead to the formation of the opposite enantiomer of the alkylation product **11**. As for complex **19**, the fastest react-

ing isomer is **A**. Therefore the fact that the enantioselectivity was lower when the Pd/**3d** catalyst was used (*ees* of up to 71%) than when the Pd/**3a** catalyst was used (*ees* of up to 96%) may be due to the decrease in the amounts of species that provide the *S* enantiomer (**A** and **C**) relative to the ones that provide (*R*)-**11** (**B**) compared with the population observed for complex **19**.

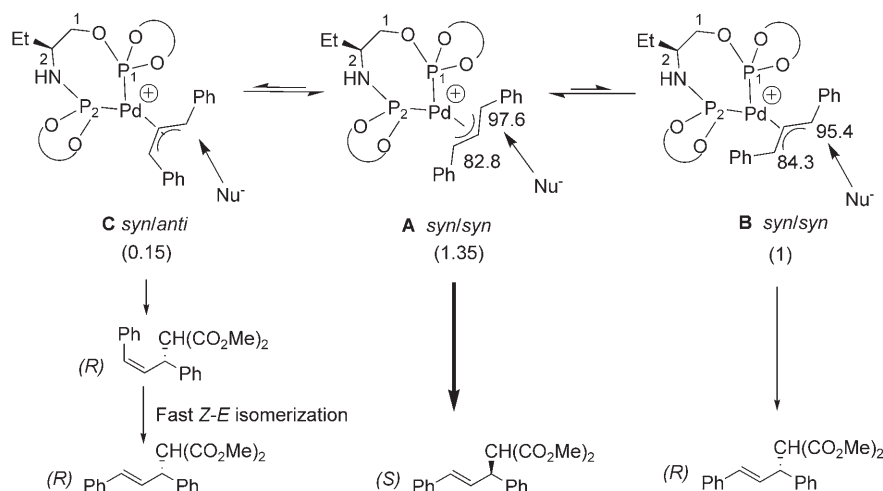
To provide further evidence that the *syn-anti* isomerism observed in complex **20** is caused by atropoisomerism of the biphenyl moieties, we studied the Pd-allyl intermediate [Pd(η^3 -1,3-diphenylallyl)-(**3f**)]BF₄ (**21**) which contains the enantiopure (*R*)-binaphthyl ligand **3f**. As for complex **19**, VT-NMR experiments indicated the presence of a mixture of two *syn/syn* isomers in a 2.2:1 ratio (see the Experimental Section) in which the more electrophilic allylic carbon termini are *trans* to the phosphoramidite moiety (Scheme 5). Assuming that the nucleophilic attack takes place at the more electrophilic carbon terminus and on the basis of the observed stereochemical outcome of the reaction, 94% (*S*) in product **11**, and the fact that the enantiomeric excess of the alkylation product **11** is higher than the diastereoisomeric excesses of the palladium intermediates, the **A** isomer must react faster than the **B** isomer, as for complex **19**.

We next studied the Pd- π -allyl intermediate [Pd(η^3 -1,3-diphenylallyl)(**6a**)]BF₄ (**22**) in which ligand **6a** is only substituted at C-2 of the amino alcohol backbone. The NMR study at room temperature revealed a mixture of two iso-



Scheme 5. Diastereoisomeric Pd-allyl intermediates for the reaction of **S1** with ligand **3f**. The relative amounts of each isomer are given in parentheses. The chemical shifts [ppm] of the allylic terminal carbon atoms are shown.

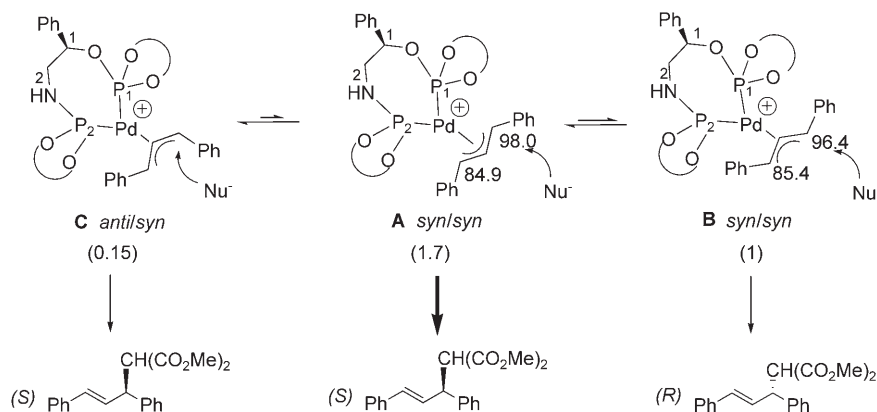
mers in a ratio of 1.5:1 (see the Experimental Section). The minor isomer was assigned by NOE experiments to the *syn/syn* isomer **B** (Scheme 6). However, for the major isomer **A**,



Scheme 6. Diastereoisomeric Pd-allyl intermediates for the reaction of **S1** with ligand **6a**. The relative amounts of each isomer are given in parentheses. The chemical shifts [ppm] of the allylic terminal carbon atoms at room temperature are shown.

and unlike **19** and **21**, the VT-³¹P NMR experiments indicated that the phosphorus atom next to C-1 (P-1, assigned by ³¹P-¹H HMBC correlation experiments) showed fluxional behaviour and was frozen out at -50°C. This fluxionality has been attributed to an equilibrium between *syn/syn* (**A**) and *syn/anti* (**C**) isomers (Scheme 6). The absence of a substituent at the C-1 position of the amino alcohol backbone favoured the atropoisomerism of the biphenyl phosphite moiety which causes an increase in the steric hindrance between the biaryl group attached to P-1 and one of the phenyl substituents of **S1**. The formation of the *syn/anti* **C** isomer minimised this new steric repulsion (Scheme 6). Note that this *syn-anti* isomerism is observed in the most electrophilic allylic terminal carbon atom (the one with the highest ¹³C chemical shifts). Assuming that the nucleophilic attack takes place at the most electrophilic carbon atom, attack at the *syn/syn* isomer **A** will lead to the formation of (*S*)-**11** whereas attack at the *syn/anti* isomer **C**, as in the attack at the **B** isomer, will lead to the formation of the opposite enantiomer of the alkylation product **11**. Therefore the considerably lower enantioselectivities observed when the Pd/**6a** catalysts were used in comparison with the Pd/**3a** catalyst system can be attributed to the presence of a *syn/syn* and *syn/anti* equilibrium for the major and more reactive Pd/**6a** catalyst intermediate. By comparing the studies of the Pd- π -allyl intermediates **19**–**22** we can conclude that a substituent is required at C-1 of the amino alcohol backbone to prevent *syn-anti* equilibration of the most electrophilic/reactive allylic carbon atom and therefore to provide high enantiomeric excesses.

Finally, the NMR study of the Pd-allyl intermediate **23** containing ligand **9a**, which is only substituted at C-1 of the amino alcohol backbone and provides enantioselectivities between those obtained with disubstituted ligand **3a** and ligand **6a** monosubstituted at the C-2 position, revealed a mixture of three isomers in a ratio of 1.7:1:0.15. The major isomers (**A** and **B**) were assigned by NOE experiments to the two *syn/syn* *endo* and *exo* isomers, whereas the minor isomer was attributed to the *anti/syn* isomer **C** (Scheme 7).



Scheme 7. Diastereoisomeric Pd-allyl intermediates for the reaction of **S1** with ligand **9a**. The relative amounts of each isomer are given in parentheses. The chemical shifts [ppm] of the allylic terminal carbon atoms are shown.

Again, this *syn/syn*–*syn/anti* equilibrium is due to the atropisomerism of the biphenyl moiety. However, in contrast to complex **22**, the VT-³¹P NMR spectra indicated fluxional behaviour of the phosphorus atom next to C-2 (phosphoramidite moiety). This can be attributed to the lack of substituents at C-2. Therefore this *syn*–*anti* isomerism is observed in the less electrophilic allylic terminal carbon atom and it has little effect on the product outcome of the reaction.

In summary, the study of the Pd-1,3-diphenylallyl intermediates indicates that nucleophilic attack takes place *trans* to the phosphoramidite moiety, that is, at the terminal allylic carbon atom next to the phosphite moiety. It has also shown that substituents need to be present on both carbon atoms of the amino alcohol backbone and in the *para* position of the biphenyl moieties to fix the configuration of the biaryl moieties and therefore to prevent the formation of complex mixtures of *syn/syn* and *syn/anti* isomers and to obtain high enantioselectivities.

Palladium 1,3-dimethylallyl complexes: When the phosphite-phosphoramidite ligand library **1–10 a–f** was used in the allylic substitution of unhin-

dered linear **S3** and cyclic **S4** substrates, the results revealed a different trend with regard the effect of the substituents on the amino alcohol ligand backbone compared with those observed with the hindered substrates **S1** and **S2**. Therefore the presence of a methyl substituent on the stereogenic carbon atom C-2 in the ligand backbone has a negative effect on the enantioselectivity of the reaction. To understand this catalytic behaviour we studied the Pd- π -allyl complexes **24** and **25** which contain ligands **1a** and **2a**, respectively. Thus, although ligand **1a**, which contains a phenyl substituent at C-2, provided high enantioselectivities (Table 3, entries 1 and 21, *ees* of up to 82% (*S*)), ligand **2a**, which contains a methyl substituent at C-2, was less enantioselective (Table 3, entry 12, *ees* of up to 45% (*S*)).

For both Pd-1,3-dimethylallyl intermediates **24** and **25**, the VT-NMR (35 °C to –80 °C) study indicated the presence of a mixture of two isomers (**A** and **B**) in a 1.85:1 ratio (see the Experimental Section). All species were assigned by NOE experiments to the *syn/syn* isomers. Unfortunately, the NMR data did not allow us to assign the major (**A**) and minor (**B**) isomers to each one of both the *endo* and *exo* *syn/syn* isomers. However, as for the 1,3-diphenylallyl intermediates, ¹³C, HSQC and HMBC NMR data indicate that the more electrophilic allylic carbon atom is *trans* to the phosphoramidite moiety in the major isomers (**24A** and **25A**). However, as isomers **24A** and **24B** show the same population and electronic properties at the allyl fragment as isomers **25A** and **25B** (Table 6), respectively, the difference in enantioselectivity observed between the Pd/**1a** and Pd/**2a** catalysts cannot be explained by the reactivity of the nucleophile towards the different π -allyl intermediates.

A plausible explanation can be found either in the enhancement of the steric interaction upon attack of the nucleophile as a result of the formation of a more bulky chiral

Table 6. Selected ¹³C NMR data for the allylic carbon atoms of complexes **24** and **25**.

	R	C-1 ^a	C-2 ^a	C-3 ^a
24A	Ph	93.9 (dd, <i>J</i> = 39.4, <i>J</i> = 7.6 Hz)	125.0 (m)	87.0 (dd, <i>J</i> = 37.2, <i>J</i> = 7.6 Hz)
24B	Ph	92.2 (dd, <i>J</i> = 35.6, <i>J</i> = 8.3 Hz)	124.3 (m)	87.0 (dd, <i>J</i> = 42.5, <i>J</i> = 5.3 Hz)
25A	Me	93.6 (dd, <i>J</i> = 40.2, <i>J</i> = 7.1 Hz)	124.6 (m)	90.0 (m)
25B	Me	90.0 (m)	124.0 (m)	87.0 (dd, <i>J</i> = 38.8, <i>J</i> = 8.6 Hz)

pocket or in a late transition state. It is known that nucleophilic substitution of the Pd-1,3-allyl cationic complex to form the Pd-olefin complex must be accompanied by rotation. A study of the models indicated that for palladium intermediate **24** the rotation is more favoured by the M isomer which would lead to the formation of the (*S*)-**14** enantiomer and explain the good *ees* obtained with this catalyst system (Figure 7). However, for palladium intermediate

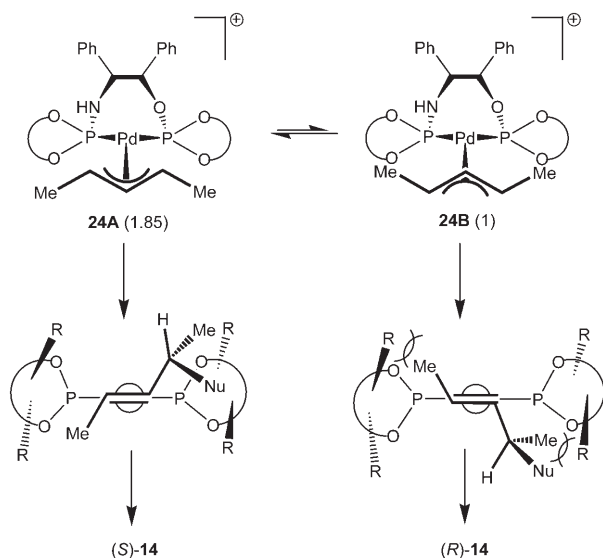


Figure 7. Steric interactions upon attack of the nucleophile in palladium intermediates **24**. The boat conformation of the seven-membered chelate ring is shown.

25, the rotation is more favoured by the W isomer which leads to the formation of (*R*)-**14** (Figure 8) and explains its lower enantioselectivity. This different behaviour is caused

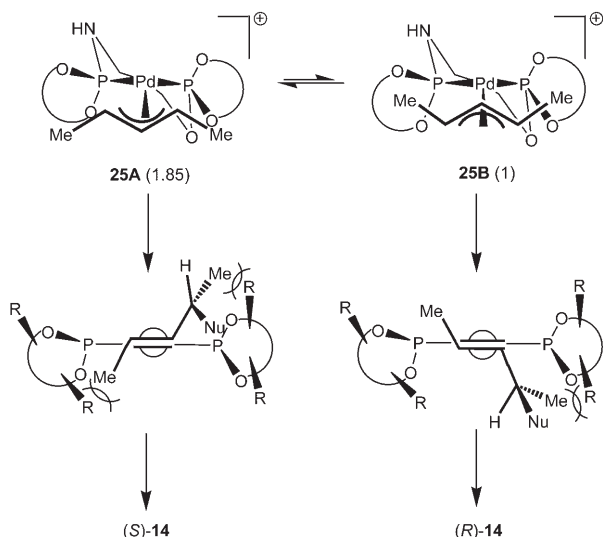


Figure 8. Steric interactions upon attack of the nucleophile in palladium intermediates **25**. The twist-boat conformation of the seven-membered chelate ring is shown.

by the fact that replacing the phenyl at C-2 by a methyl substituent produces a change in the conformation of the seven-membered chelate ring from a boat to a twisted-boat conformation which affects the chiral pocket around the metal centre. These results also suggest that the major isomers **24A** and **25A** correspond to the *syn/syn* M isomers whereas the isomers **24B** and **25B** correspond to the *syn/syn* W isomers.

Conclusions

A library of phosphite-phosphoramidite ligands **1–10a–f** have been synthesised for the palladium-catalysed allylic substitution reactions of several substrates with different electronic and steric properties. These ligands have three main advantages: 1) they can be prepared in one step from readily available chiral 1,2-amino alcohols, 2) their π -acceptor character increases reaction rates and 3) their modular nature enables the substituents/configurations of the amino alcohol backbone (C-1 and C-2), the amino group and the biaryl moieties to be easily and systematically varied. Thus, by carefully selecting the ligand components, high enantioselectivities (*ees* of up to 99%) and activities (TOFs of up to 800 mol substrate/(mol Pd h)⁻¹) have been achieved for a wide range of substrates with different steric and electronic properties. In general, the activities are mainly affected by the substituents in the biaryl groups, whereas the enantioselectivities are highly affected by the substituents and the axial chirality of the biaryl moieties and the substituents/configurations in the amino alcohol backbone. However, the effect of these parameters depends on each substrate class. Note that both enantiomers of the product can be obtained with high enantioselectivities simply by changing the absolute configuration of either the biaryl moieties or the amino alcohol unit.

The study of the Pd- π -1,3-diphenylallyl and Pd- π -1,3-dimethylallyl intermediates by NMR spectroscopy has allowed the observed catalytic behaviour to be understood. This study indicates that nucleophilic attack takes place predominantly at the allylic terminal carbon atom located *trans* to the phosphoramidite moiety. The study of the Pd-1,3-diphenylallyl intermediate also indicates that substituents need to be present at both carbon atoms of the amino alcohol backbone and in the *para* position of the biphenyl moieties to fix the configuration of the biaryl moieties and therefore to prevent the formation of complex mixtures of *syn/syn* and *syn/anti* isomers and to obtain high enantioselectivities. However, for the Pd-1,3-methylallyl intermediates the difference in enantioselectivity observed cannot be explained by the reactivity of the nucleophile towards the different π -allyl intermediates. We found that the enhancement of the steric interaction upon attack of the nucleophile to be a good explanation.

To sum up, the combination of high enantioselectivities (*ees* of up to 99%), high activities and high substrate versatility, and the low cost of the ligands means that it may be

possible to use readily available and highly modular 1,2-amino alcohol based phosphite-phosphoramidite ligands in the allylic substitution of a wide range of substrates. The efficiency of this ligand design is also corroborated by the fact that these Pd-phosphite-phosphoramidite catalysts provide higher activity and enantioselectivity than their 1,2-diphosphite and phosphinite-aminophosphine analogues. The potential usefulness of this new type of ligand in other catalytic reactions is currently being studied.

Experimental Section

General: All reactions were carried out by using standard Schlenk techniques under argon. Solvents were purified and dried by standard procedures. The phosphorochloridites were readily prepared in one step from the corresponding biaryls.^[18] ¹H, ¹³C{¹H} and ³¹P{¹H} NMR spectra were recorded with a 400 MHz spectrometer. Chemical shifts are reported relative to that of SiMe₄ (¹H and ¹³C) as internal standard or H₃PO₄ (³¹P) as external standard. ¹H, ¹³C and ³¹P assignments were made based on ¹H-¹H gCOSY, ¹H-¹³C gHSQC and ¹H-³¹P gHMBC experiments.

General procedure for the preparation of ligands 1–10a–f: Phosphorochloridite (2.2 mmol) produced in situ was dissolved in toluene (5 mL) and pyridine (0.36 mL, 4.6 mmol) was added. Amino alcohol (1 mmol) was azeotropically dried with toluene (3 × 1 mL) and then dissolved in toluene (10 mL) and pyridine (0.36 mL, 4.6 mmol) was added. The phosphorochloridite solution was transferred slowly at 0°C to the solution of the amino alcohol. The reaction mixture was warmed up to 80°C and stirred overnight and then the pyridine salts were removed by filtration. Evaporation of the solvent gave a white foam which was purified by flash chromatography (toluene/NEt₃=100:1) to produce the corresponding ligand as a white powder.

1a: Yield: 0.67 g, 62%. ¹H NMR (C₆D₆): δ = 1.23 (s, 9H; CH₃, *t*Bu), 1.24 (s, 9H; CH₃, *t*Bu), 1.35 (s, 9H; CH₃, *t*Bu), 1.36 (s, 9H; CH₃, *t*Bu), 1.37 (s, 9H; CH₃, *t*Bu), 1.39 (s, 9H; CH₃, *t*Bu), 1.40 (s, 18H; CH₃, *t*Bu), 3.66 (m, 1H; NH), 4.81 (m, 1H; CH-N), 5.23 (m, 1H; CH-O), 6.35–7.50 ppm (m, 18H; CH=); ¹³C NMR (C₆D₆): δ = 31.1 (CH₃, *t*Bu), 31.2 (CH₃, *t*Bu), 31.4 (CH₃, *t*Bu), 31.8 (CH₃, *t*Bu), 34.8 (C, *t*Bu), 34.9 (C, *t*Bu), 35.4 (C, *t*Bu), 35.5 (C, *t*Bu), 60.6 (d, CH-N, ³J_{C-P} = 16.7 Hz), 82.1 (CH-O), 124.2 (CH=), 124.3 (CH=), 124.4 (CH=), 124.6 (CH=), 125.5 (CH=), 126.2 (CH=), 126.4 (CH=), 126.5 (CH=), 126.6 (CH=), 126.9 (CH=), 127.2 (CH=), 127.5 (CH=), 127.6 (CH=), 127.8 (CH=), 128.2 (CH=), 128.3 (CH=), 128.5 (CH=), 129.4 (CH=), 132.8 (C), 133.1 (C), 133.4 (C), 136.8 (C), 138.5 (C), 139.9 (C), 140.2 (C), 140.5 (C), 145.9 (C), 146.0 (C), 146.3 (C), 146.6 ppm (C); ³¹P NMR (C₆D₆): δ = 143.9 (br), 151.2 ppm (s); elemental analysis calcd (%) for C₇₀H₉₃NO₃P₂: C 77.10, H 8.60, N 1.28; found: C 77.01, H 8.62, N 1.33.

1b: Yield: 0.60 g, 61%. ¹H NMR (C₇D₈): δ = 1.21 (s, 9H; CH₃, *t*Bu), 1.25 (s, 9H; CH₃, *t*Bu), 1.46 (s, 9H; CH₃, *t*Bu), 1.55 (s, 9H; CH₃, *t*Bu), 3.29 (s, 3H; OCH₃), 3.31 (s, 9H; OCH₃), 3.83 (m, 1H; NH), 5.21 (m, 1H; CH-N), 5.48 (m, 1H; CH-O), 6.47–7.08 ppm (m, 18H; CH=); ¹³C NMR (C₇D₈): δ = 30.7 (CH₃, *t*Bu), 31.1 (CH₃, *t*Bu), 35.2 (C, *t*Bu), 35.3 (C, *t*Bu), 35.4 (C, *t*Bu), 35.5 (C, *t*Bu), 54.7 (OCH₃), 54.8 (OCH₃), 60.8 (d, ³J_{C-P} = 19 Hz; CH-N), 82.6 (CH-O), 112.6 (CH=), 112.8 (CH=), 112.9 (CH=), 113.1 (CH=), 114.3 (CH=), 114.4 (CH=), 114.5 (CH=), 114.6 (CH=), 124.7 (CH=), 124.9 (CH=), 125.1 (CH=), 125.4 (CH=), 127.5 (CH=), 127.7 (CH=), 128.1 (CH=), 128.2 (CH=), 128.7 (CH=), 128.9 (CH=), 133.9 (C), 134.3 (C), 134.5 (C), 134.6 (C), 136.8 (C), 137.3 (C), 138.9 (C), 142.3 (C), 142.7 (C), 142.8 (C), 155.8 (C), 156.0 (C), 156.1 (C), 156.3 ppm (C); ³¹P NMR (C₇D₈): δ = 143.3 (br), 151.8 ppm (s); elemental analysis calcd (%) for C₃₈H₆₉NO₃P₂: C 70.64, H 7.05, N 1.42; found: C 70.43, H 6.96, N 1.39.

1c: Yield: 0.37 g, 58%. ¹H NMR (C₆D₆): δ = 4.21 (m, 1H; NH), 4.86 (m, 1H; CH-N), 5.73 (m, 1H; CH-O), 6.70–7.23 ppm (m, 26H; CH=); ¹³C NMR (C₆D₆): δ = 60.7 (m; CH-N), 81.6 (m; CH-O), 122.7 (CH=),

122.8 (CH=), 123.1 (CH=), 125.1 (CH=), 125.2 (CH=), 125.6 (CH=), 125.7 (CH=), 126.0 (CH=), 127.7 (CH=), 127.9 (CH=), 128.4 (CH=), 128.6 (CH=), 128.9 (CH=), 129.6 (CH=), 129.8 (CH=), 130.2 (CH=), 130.3 (CH=), 130.4 (CH=), 130.6 (CH=), 131.6 (C), 132.0 (C), 132.2 (C), 132.6 (C), 138.7 (C), 139.9 (C), 150.2 (C), 150.6 (C), 151.3 (C), 151.6 ppm (C); ³¹P NMR (C₆D₆): δ = 142.8 (s), 149.7 ppm (s); elemental analysis calcd (%) for C₃₈H₂₉NO₃P₂: C 71.14, H 4.56, N 2.18; found: C 71.06, H 4.59, N 2.21.

1d: Yield: 0.45 g, 48%. ¹H NMR (C₆D₆): δ = 0.25 (s, 9H; CH₃-Si), 0.29 (s, 9H; CH₃-Si), 0.37 (s, 9H; CH₃-Si), 0.39 (s, 9H; CH₃-Si), 3.79 (s, 1H; NH), 4.96 (m, 1H; CH-N), 5.71 (m, 1H; CH-O), 6.40–7.40 ppm (m, 22H; CH=); ¹³C NMR (C₆D₆): δ = 0.4 (CH₃-Si), 0.6 (CH₃-Si), 0.7 (CH₃-Si), 61.6 (d, J_{C-P} = 12.8 Hz; CH-N), 83.1 (CH-O), 124.8 (CH=), 125.1 (CH=), 125.3 (CH=), 125.7 (CH=), 126.0 (C), 127.9 (CH=), 128.1 (CH=), 128.4 (CH=), 128.8 (CH=), 131.5 (C), 132.1 (C), 132.5 (CH=), 132.7 (CH=), 133.0 (CH=), 133.4 (CH=), 135.4 (CH=), 135.6 (CH=), 135.8 (CH=), 135.9 (CH=), 137.2 (C), 138.2 (C), 138.8 (C), 155.3 (C), 155.5 (C), 156.3 (C), 156.7 ppm (C); ³¹P NMR (C₆D₆): δ = 146.9 (br), 153.5 ppm (s); elemental analysis calcd (%) for C₅₀H₆₁NO₃P₂Si₄: C 64.55, H 6.61, N 1.51; found: C 64.59, H 6.64, N 1.54.

1e: Yield: 0.24 g, 21%. ¹H NMR (C₆D₆): δ = 0.11 (s, 9H; CH₃-Si), 0.14 (s, 9H; CH₃-Si), 0.64 (s, 9H; CH₃-Si), 0.70 (s, 9H; CH₃-Si), 3.90 (s, 1H; CH-N), 4.12 (m, 1H; NH), 6.01 (m, 1H; CH-O), 6.20–8.20 ppm (m, 30H; CH=); ¹³C NMR (C₆D₆): δ = 0.4 (CH₃-Si), 0.5 (CH₃-Si), 0.7 (CH₃-Si), 61.8 (d, CH-N, J_{C-P} = 13.2 Hz), 83.2 (CH-O), 124.9 (CH=), 125.0 (CH=), 125.2 (CH=), 125.6 (CH=), 126.0 (C), 127.8 (CH=), 128.2 (CH=), 128.5 (CH=), 128.8 (CH=), 131.4 (C), 132.3 (C), 132.4 (CH=), 132.9 (CH=), 133.0 (CH=), 133.4 (CH=), 135.6 (CH=), 135.7 (CH=), 135.8 (CH=), 135.9 (CH=), 137.2 (C), 138.2 (C), 138.8 (C), 155.4 (C), 155.6 (C), 156.5 (C), 156.9 ppm (C); ³¹P NMR (C₆D₆): δ = 149.5 (s), 160.7 ppm (s); elemental analysis calcd (%) for C₆₆H₆₉NO₃P₂Si₄: C 70.12, H 6.15, N 1.24; found: C 70.23, H 6.21, N 1.21.

1f: Yield: 0.20 g, 18%. ¹H NMR (C₆D₆): δ = 0.09 (s, 9H; CH₃-Si), 0.11 (s, 9H; CH₃-Si), 0.76 (s, 9H; CH₃-Si), 0.89 (s, 9H; CH₃-Si), 3.20 (s, 1H; NH), 4.87 (m, 1H; CH-N), 5.63 (m, 1H; CH-O), 6.40–8.40 ppm (m, 30H; CH=); ¹³C NMR (C₆D₆): δ = 0.0 (CH₃-Si), 0.4 (CH₃-Si), 0.6 (CH₃-Si), 0.9 (CH₃-Si), 60.8 (d, J_{C-P} = 30.2 Hz; CH-N), 83.8 (d, J_{C-P} = 9.2 Hz; CH-O), 123.7 (CH=), 124.0 (CH=), 125.1 (CH=), 125.2 (CH=), 125.5 (CH=), 126.0 (C), 126.9 (CH=), 127.1 (C), 127.2 (CH=), 127.3 (CH=), 127.5 (CH=), 128.2 (CH=), 128.5 (CH=), 128.8 (CH=), 129.1 (CH=), 129.2 (CH=), 130.3 (C), 131.1 (CH=), 131.4 (CH=), 131.8 (CH=), 132.9 (CH=), 133.3 (CH=), 133.5 (CH=), 134.0 (CH=), 134.2 (C), 134.8 (CH=), 135.1 (CH=), 135.2 (CH=), 136.0 (CH=), 137.6 (C), 137.8 (CH=), 138.3 (CH=), 139.7 (C), 139.8 (C), 151.9 (C), 153.3 (C), 153.6 (C), 154.9 ppm (C); ³¹P NMR (C₆D₆): δ = 136.8 (s), 157.8 ppm (s); elemental analysis calcd (%) for C₆₆H₆₉NO₃P₂Si₄: C 70.12, H 6.15, N 1.24; found: C 70.44, H 6.32, N 1.31.

2a: Yield: 0.67 g, 65%. ¹H NMR (C₇D₈): δ = 0.77 (d, ³J_{H-H} = 6.4 Hz, 3H; CH₃), 1.26 (s, 9H; CH₃, *t*Bu), 1.28 (s, 18H; CH₃, *t*Bu), 1.30 (s, 9H; CH₃, *t*Bu), 1.40 (s, 9H; CH₃, *t*Bu), 1.45 (s, 9H; CH₃, *t*Bu), 1.56 (s, 9H; CH₃, *t*Bu), 1.66 (s, 9H; CH₃, *t*Bu), 3.29 (m, 1H; NH), 3.80 (br, 1H; CH-N), 5.48 (m, 1H; CH-O), 6.97–7.59 ppm (m, 13H; CH=); ¹³C NMR (C₇D₈): δ = 31.1 (CH₃, *t*Bu), 31.3 (CH₃, *t*Bu), 31.5 (CH₃, *t*Bu), 31.6 (CH₃, *t*Bu), 31.7 (CH₃, *t*Bu), 34.6 (C, *t*Bu), 35.5 (C, *t*Bu), 35.6 (C, *t*Bu), 35.7 (C, *t*Bu), 52.8 (d, ³J_{C-P} = 12.4 Hz; CH-N), 82.2 (CH-O), 124.1 (CH=), 124.3 (CH=), 124.8 (CH=), 125.1 (CH=), 125.3 (CH=), 125.6 (CH=), 126.6 (CH=), 126.7 (CH=), 126.9 (CH=), 127.9 (CH=), 128.0 (CH=), 128.1 (CH=), 128.6 (CH=), 128.8 (CH=), 129.0 (CH=), 129.2 (CH=), 133.2 (C), 133.9 (C), 137.4 (C), 138.8 (C), 140.2 (C), 140.6 (C), 140.8 (C), 145.9 (C), 146.2 (C), 146.3 (C), 146.8 ppm (C); ³¹P NMR (C₇D₈): δ = 144.9 (br), 150.3 ppm (s); elemental analysis calcd (%) for C₆₅H₉₁NO₃P₂: C 75.92, H 8.92, N 1.36; found: C 75.89, H 8.95, N 1.33.

3a: Yield: 0.77 g, 71%. ¹H NMR (CDCl₃): δ = 1.23 (s, 9H; CH₃, *t*Bu), 1.24 (s, 9H; CH₃, *t*Bu), 1.35 (s, 9H; CH₃, *t*Bu), 1.36 (s, 9H; CH₃, *t*Bu), 1.37 (s, 9H; CH₃, *t*Bu), 1.40 (s, 9H; CH₃, *t*Bu), 1.41 (s, 18H; CH₃, *t*Bu), 3.66 (m, 1H; NH), 4.81 (m, 1H; CH-N), 5.23 (m, 1H; CH-O), 6.35–7.50 ppm (m, 18H; CH=); ¹³C NMR (CDCl₃): δ = 31.1 (CH₃, *t*Bu), 31.2 (CH₃, *t*Bu), 31.4 (CH₃, *t*Bu), 31.8 (CH₃, *t*Bu), 34.8 (C, *t*Bu), 34.9 (C, *t*Bu), 35.4 (C, *t*Bu), 35.5 (C, *t*Bu), 60.6 (d, ³J_{C-P} = 18.3 Hz; CH-N), 82.1 (CH-O),

124.2 (CH=), 124.3 (CH=), 124.4 (CH=), 124.6 (CH=), 125.5 (CH=), 126.2 (CH=), 126.4 (CH=), 126.5 (CH=), 126.6 (CH=), 126.9 (CH=), 127.2 (CH=), 127.5 (CH=), 127.6 (CH=), 127.8 (CH=), 128.2 (CH=), 128.4 (CH=), 129.3 (CH=), 132.8 (C), 133.1 (C), 133.3 (C), 133.4 (C), 136.8 (C), 138.1 (C), 138.5 (C), 139.9 (C), 140.5 (C), 145.9 (C), 146.2 (C), 146.6 ppm (C); ^{31}P NMR (CDCl_3): δ = 143.9 (br), 151.2 ppm (s); elemental analysis calcd (%) for $\text{C}_{70}\text{H}_{93}\text{NO}_5\text{P}_2$: C 77.10, H 8.60, N 1.28; found: C 77.12, H 8.61, N 1.31.

3d: Yield: 0.34 g, 36%. ^1H NMR (C_6D_6): δ = 0.25 (s, 9H; CH_3 -Si), 0.29 (s, 9H; CH_3 -Si), 0.37 (s, 9H; CH_3 -Si), 0.39 (s, 9H; CH_3 -Si), 3.79 (s, 1H; NH), 4.96 (m, 1H; CH-N), 5.71 (m, 1H; CH-O), 6.40–7.40 ppm (m, 22H; CH=); ^{13}C NMR (C_6D_6): δ = 0.4 (CH_3 -Si), 0.6 (CH_3 -Si), 0.7 (CH_3 -Si), 61.6 (d, $J_{\text{C-P}}$ = 12.8 Hz; CH-N), 83.1 (CH-O), 124.8 (CH=), 125.1 (CH=), 125.3 (CH=), 125.7 (CH=), 126.0 (C), 127.9 (CH=), 128.1 (CH=), 128.4 (CH=), 128.8 (CH=), 131.5 (C), 132.1 (C), 132.5 (CH=), 132.7 (CH=), 133.0 (CH=), 133.4 (CH=), 135.4 (CH=), 135.6 (CH=), 135.8 (CH=), 135.9 (CH=), 137.2 (C), 138.2 (C), 138.8 (C), 155.3 (C), 155.5 (C), 156.3 (C), 156.7 ppm (C); ^{31}P NMR (C_6D_6): δ = 146.9 (br), 153.5 ppm (s); elemental analysis calcd (%) for $\text{C}_{50}\text{H}_{61}\text{NO}_3\text{P}_2\text{Si}_4$: C 64.55, H 6.61, N 1.51; found: C 64.57, H 6.70, N 1.58.

3f: Yield: 0.22 g, 20%. ^1H NMR (C_6D_6): δ = 0.11 (s, 9H; CH_3 -Si), 0.12 (s, 9H; CH_3 -Si), 0.79 (s, 9H; CH_3 -Si), 0.92 (s, 9H; CH_3 -Si), 3.45 (s, 1H; NH), 4.76 (m, 1H; CH-N), 5.34 (m, 1H; CH-O), 6.40–8.40 ppm (m, 30H; CH=); ^{13}C NMR (C_6D_6): δ = 0.2 (CH_3 -Si), 0.6 (CH_3 -Si), 0.9 (CH_3 -Si), 61.8 (d, $J_{\text{C-P}}$ = 22.4 Hz; CH-N), 84.2 (CH-O), 124.1 (CH=), 124.3 (CH=), 125.2 (CH=), 125.4 (CH=), 125.9 (CH=), 127.0 (C), 127.1 (CH=), 127.2 (C), 127.5 (CH=), 127.6 (CH=), 127.7 (CH=), 128.5 (CH=), 128.7 (CH=), 129.0 (CH=), 129.2 (CH=), 129.3 (CH=), 130.4 (C), 131.1 (CH=), 131.6 (CH=), 131.9 (CH=), 132.3 (CH=), 133.5 (CH=), 133.6 (CH=), 134.3 (CH=), 134.7 (C), 134.8 (CH=), 135.3 (CH=), 136.2 (CH=), 137.8 (C), 138.3 (CH=), 139.2 (CH=), 139.3 (C), 139.5 (C), 152.9 (C), 153.4 (C), 154.3 (C), 154.7 ppm (C); ^{31}P NMR (C_6D_6): δ = 136.9 (s), 159.2 ppm (s); elemental analysis calcd (%) for $\text{C}_{66}\text{H}_{69}\text{NO}_3\text{P}_2\text{Si}_4$: C 70.12, H 6.15, N 1.24; found: C 70.22, H 6.12, N 1.26.

4a: Yield: 0.2 g, 20%. ^1H NMR (C_6D_6): δ = 1.20 (s, 9H; CH_3 , *t*Bu), 1.23 (m, 3H; CH_3), 1.24 (s, 18H; CH_3 , *t*Bu), 1.25 (s, 9H; CH_3 , *t*Bu), 1.40 (br, 9H; CH_3 , *t*Bu), 1.46 (br, 9H; CH_3 , *t*Bu), 1.53 (br, 9H; CH_3 , *t*Bu), 1.63 (br, 9H; CH_3 , *t*Bu), 2.26 (br, 1H; CH_3 -N), 4.27 (br, 1H; CH-N), 5.44 (br, 1H; CH-O), 6.95–7.6 ppm (m, 13H; CH=); ^{13}C NMR (C_7D_8): δ = 31.3 (CH_3 , *t*Bu), 31.4 (CH_3 , *t*Bu), 31.6 (CH_3 , *t*Bu), 31.9 (CH_3 , *t*Bu), 34.6 (C, *t*Bu), 35.5 (C, *t*Bu), 35.6 (C, *t*Bu), 36.5 (CH_3 -N), 53.2 (br, CH-N), 82.0 (br, CH-O), 124.1 (CH=), 124.4 (CH=), 124.9 (CH=), 125.1 (CH=), 125.3 (CH=), 125.6 (CH=), 126.6 (CH=), 126.7 (CH=), 126.9 (CH=), 127.9 (CH=), 128.4 (CH=), 128.5 (CH=), 128.6 (CH=), 128.8 (CH=), 129.0 (CH=), 129.3 (CH=), 133.2 (C), 133.9 (C), 137.4 (C), 138.8 (C), 140.2 (C), 140.6 (C), 140.8 (C), 146.0 (C), 146.3 (C), 146.4 (C), 146.9 ppm (C); ^{31}P NMR (C_6D_6): δ = 145.1 (br), 148.2 ppm (s); elemental analysis calcd (%) for $\text{C}_{66}\text{H}_{93}\text{NO}_3\text{P}_2$: C 76.05, H 8.99, N 1.34; found: C 76.11, H 9.02, N 1.37.

5a: Yield: 0.63 g, 62%. ^1H NMR (CDCl_3): δ = 1.27 (s, 9H; CH_3 , *t*Bu), 1.35 (s, 9H; CH_3 , *t*Bu), 1.36 (s, 9H; CH_3 , *t*Bu), 1.37 (s, 9H; CH_3 , *t*Bu), 1.38 (s, 9H; CH_3 , *t*Bu), 1.41 (s, 9H; CH_3 , *t*Bu), 1.42 (s, 9H; CH_3 , *t*Bu), 1.43 (s, 9H; CH_3 , *t*Bu), 3.68 (m, 1H; NH), 3.80 (m, 1H; CH_2 -O), 3.87 (m, 1H; CH_2 -O), 4.36 (m, 1H; CH-N), 6.90–7.50 ppm (m, 13H; CH=); ^{13}C NMR (CDCl_3): δ = 31.1 (CH_3 , *t*Bu), 31.2 (CH_3 , *t*Bu), 31.3 (CH_3 , *t*Bu), 31.5 (CH_3 , *t*Bu), 31.6 (CH_3 , *t*Bu), 31.7 (CH_3 , *t*Bu), 31.8 (CH_3 , *t*Bu), 31.9 (CH_3 , *t*Bu), 35.4 (C, *t*Bu), 35.4 (C, *t*Bu), 35.5 (C, *t*Bu), 35.6 (C, *t*Bu), 56.0 (m; CH-N), 68.8 (m; CH-O), 124.1 (CH=), 124.3 (CH=), 124.4 (CH=), 124.5 (CH=), 126.2 (CH=), 126.6 (CH=), 126.7 (CH=), 127.5 (CH=), 127.6 (CH=), 128.4 (CH=), 128.5 (CH=), 129.3 (CH=), 132.8 (C), 133.1 (C), 133.7 (C), 138.1 (C), 139.9 (C), 140.2 (C), 140.4 (C), 141.1 (C), 145.8 (C), 146.1 (C), 146.3 (C), 146.4 (C), 146.6 (C), 146.9 (C), 147.1 ppm (C); ^{31}P NMR (CDCl_3): δ = 137.7 (s), 148.6 ppm (s); elemental analysis calcd (%) for $\text{C}_{64}\text{H}_{89}\text{NO}_3\text{P}_2$: C 75.78, H 8.84, N 1.38; found: C 76.01, H 8.91, N 1.37.

6a: Yield: 0.57 g, 59%. ^1H NMR (CDCl_3): δ = 0.66 (t, $^3J_{\text{H-H}}$ = 7.6 Hz, 3H; CH_3), 1.35 (s, 9H; CH_3 , *t*Bu), 1.36 (s, 9H; CH_3 , *t*Bu), 1.37 (s, 18H; CH_3 , *t*Bu), 1.46 (s, 9H; CH_3 , *t*Bu), 1.47 (s, 9H; CH_3 , *t*Bu), 1.48 (s, 18H; CH_3 ,

*t*Bu), 1.52 (m, 2H; CH_2), 3.21 (m, 1H; NH), 3.26 (m, 1H; CH-N), 3.62 (m, 1H; CH_2 -O), 3.82 (m, 1H; CH_2 -O), 7.10–7.50 ppm (m, 8H; CH=); ^{13}C NMR (CDCl_3): δ = 10.6 (CH_3), 29.9 (CH_2), 31.2 (CH_3 , *t*Bu), 31.3 (CH_3 , *t*Bu), 31.4 (CH_3 , *t*Bu), 31.5 (CH_3 , *t*Bu), 31.6 (CH_3 , *t*Bu), 31.7 (CH_3 , *t*Bu), 31.8 (CH_3 , *t*Bu), 31.9 (CH_3 , *t*Bu), 34.8 (C, *t*Bu), 35.5 (C, *t*Bu), 53.1 (m; CH-N), 66.8 (m; CH-O), 124.1 (CH=), 124.3 (CH=), 124.4 (CH=), 126.2 (CH=), 126.7 (CH=), 126.8 (CH=), 132.9 (C), 133.1 (C), 133.2 (C), 139.9 (C), 140.2 (C), 140.4 (C), 146.3 (C), 146.5 (C), 146.8 (C), 147.3 ppm (C); ^{31}P NMR (CDCl_3): δ = 139.7 (s), 150.3 ppm (s); elemental analysis calcd (%) for $\text{C}_{60}\text{H}_{89}\text{NO}_3\text{P}_2$: C 74.58, H 9.28, N 1.45; found: C 74.62, H 9.31, N 1.47.

7a: Yield: 0.51 g, 52%. ^1H NMR (CDCl_3): δ = 0.71 (d, $^3J_{\text{H-H}}$ = 4.4 Hz, 3H; CH_3), 0.79 (d, $^3J_{\text{H-H}}$ = 4.4 Hz, 3H; CH_3), 1.36 (s, 18H; CH_3 , *t*Bu), 1.37 (s, 18H; CH_3 , *t*Bu), 1.45 (s, 9H; CH_3 , *t*Bu), 1.48 (s, 27H; CH_3 , *t*Bu), 1.80 (m, 1H; CH), 1.52 (m, 2H; CH_2), 3.16 (m, 1H; NH), 3.32 (m, 1H; CH-N), 3.66 (m, 1H; CH_2 -O), 3.79 (m, 1H; CH_2 -O), 7.10–7.50 ppm (m, 8H; CH=); ^{13}C NMR (CDCl_3): δ = 18.1 (CH_3), 18.7 (CH_3), 30.4 (m; CH), 31.2 (CH_3 , *t*Bu), 31.3 (CH_3 , *t*Bu), 31.4 (CH_3 , *t*Bu), 31.5 (CH_3 , *t*Bu), 31.7 (CH_3 , *t*Bu), 31.8 (CH_3 , *t*Bu), 34.8 (C, *t*Bu), 34.9 (C), 35.6 (C, *t*Bu), 57.2 (m; CH-N), 66.1 (m; CH-O), 124.1 (CH=), 124.3 (CH=), 124.4 (CH=), 126.4 (CH=), 126.6 (CH=), 126.7 (CH=), 132.9 (C), 133.1 (C), 133.3 (C), 140.0 (C), 140.3 (C), 145.8 (C), 145.9 (C), 146.4 (C), 147.1 ppm (C); ^{31}P NMR (CDCl_3): δ = 138.8 (s), 150.0 ppm (s); elemental analysis calcd (%) for $\text{C}_{60}\text{H}_{91}\text{NO}_3\text{P}_2$: C 74.74, H 9.36, N 1.43; found: C 74.86, H 9.42, N 1.42.

8a: Yield: 0.42 g, 42%. ^1H NMR (CDCl_3): δ = 0.90 (s, 9H; CH_3), 1.56 (s, 18H; CH_3 , *t*Bu), 1.57 (s, 18H; CH_3 , *t*Bu), 1.68 (s, 9H; CH_3 , *t*Bu), 1.69 (s, 18H; CH_3 , *t*Bu), 1.71 (s, 9H; CH_3 , *t*Bu), 3.36 (m, 1H; NH), 3.46 (m, 1H; CH-N), 3.79 (m, 1H; CH_2 -O), 4.09 (m, 1H; CH_2 -O), 7.30–7.70 ppm (m, 8H; CH=); ^{13}C NMR (CDCl_3): δ = 27.2 (CH_3), 31.4 (CH_3 , *t*Bu), 31.6 (CH_3 , *t*Bu), 31.8 (CH_3 , *t*Bu), 31.9 (CH_3 , *t*Bu), 34.8 (C, *t*Bu), 35.0 (C, *t*Bu), 35.8 (C, *t*Bu), 62.3 (m; CH-N), 66.4 (m; CH-O), 124.2 (CH=), 124.4 (CH=), 124.6 (CH=), 126.8 (CH=), 126.9 (CH=), 133.1 (C), 133.2 (C), 133.5 (C), 140.1 (C), 140.4 (C), 140.7 (C), 146.0 (C), 146.4 (C), 146.7 (C), 147.0 ppm (C); ^{31}P NMR (CDCl_3): δ = 165.0 (s), 176.5 ppm (s); elemental analysis calcd (%) for $\text{C}_{62}\text{H}_{92}\text{NO}_3\text{P}_2$: C 74.89, H 9.43, N 1.41; found: C 74.94, H 9.52, N 1.49.

9a: Yield: 0.62 g, 63%. ^1H NMR (C_6D_6): δ = 1.25 (s, 9H; CH_3 , *t*Bu), 1.29 (s, 18H; CH_3 , *t*Bu), 1.30 (s, 9H; CH_3 , *t*Bu), 1.45 (s, 9H; CH_3 , *t*Bu), 1.49 (s, 9H; CH_3 , *t*Bu), 1.53 (s, 9H; CH_3 , *t*Bu), 1.56 (s, 9H; CH_3 , *t*Bu), 3.23 (m, 3H; NH, CH_2 -N), 5.32 (m, 1H; CH-O), 6.90–7.60 ppm (m, 13H; CH=); ^{13}C NMR (C_6D_6): δ = 31.7 (CH_3 , *t*Bu), 31.9 (CH_3 , *t*Bu), 32.0 (CH_3 , *t*Bu), 35.0 (C, *t*Bu), 35.9 (C, *t*Bu), 47.9 (m; CH-N), 79.5 (m; CH-O), 124.4 (CH=), 124.7 (CH=), 124.9 (CH=), 126.0 (CH=), 126.9 (CH=), 127.1 (CH=), 127.4 (CH=), 127.7 (CH=), 128.8 (CH=), 128.9 (CH=), 129.6 (CH=), 133.8 (C), 134.2 (C), 134.4 (C), 140.0 (C), 140.8 (C), 140.9 (C), 141.0 (C), 141.2 (C), 146.5 (C), 146.6 (C), 146.9 (C), 147.3 ppm (C); ^{31}P NMR (C_6D_6): δ = 145.9 (s), 147.7 ppm (s); elemental analysis calcd (%) for $\text{C}_{64}\text{H}_{89}\text{NO}_3\text{P}_2$: C 75.78, H 8.84, N 1.38; found: C 75.81, H 8.87, N 1.43.

10f: Yield: 0.57 g, 59%. ^{31}P NMR (C_6D_6): δ = 133.8 (s), 146.9 ppm (s); ^1H NMR (C_6D_6): δ = 0.41 (s, 9H; CH_3 -Si), 0.49 (s, 9H; CH_3 -Si), 0.51 (s, 9H; CH_3 -Si), 0.55 (s, 9H; CH_3 -Si), 2.50 (m, 1H; CH_2 -N), 2.67 (m, 1H; CH_2 -N), 2.97 (m, 1H; NH), 3.11 (m, 1H; CH-O), 3.57 (m, 1H; CH-O), 6.80–8.10 ppm (m, 20H; CH=); ^{13}C NMR (C_6D_6): δ = 0.4 (CH_3 -Si), 0.6 (CH_3 -Si), 0.7 (CH_3 -Si), 41.4 (m; CH_2 -N), 66.1 (m; CH_2 -O), 125.1 (CH=), 125.4 (CH=), 126.0 (C), 127.1 (CH=), 127.2 (CH=), 127.4 (CH=), 128.8 (CH=), 128.9 (CH=), 129.0 (CH=), 129.1 (CH=), 129.2 (CH=), 129.4 (C), 129.6 (CH=), 131.2 (CH=), 131.4 (CH=), 131.8 (CH=), 132.0 (CH=), 132.4 (CH=), 133.0 (CH=), 134.7 (C), 135.0 (CH=), 135.1 (CH=), 137.5 (CH=), 137.7 (CH=), 137.8 (CH=), 138.0 (CH=), 144.8 (C), 145.3 (C), 152.6 (C), 153.5 (C), 153.6 (C), 154.4 ppm (C); elemental analysis calcd (%) for $\text{C}_{54}\text{H}_{61}\text{NO}_3\text{P}_2\text{Si}_4$: C 66.29, H 6.28, N 1.43; found: C 66.34, H 6.32, N 1.48.

General procedure for the preparation of $[\text{Pd}(\eta^3\text{-allyl})(\text{L})]\text{BF}_4$ complexes: The corresponding ligand (0.05 mmol) and the complex $[\text{Pd}(\mu\text{-Cl})(\eta^3\text{-1,3-allyl})_2]$ (0.025 mmol) were dissolved in CD_2Cl_2 (1.5 mL) at room temperature under argon. AgBF_4 (9.8 mg, 0.5 mmol) was added after 30 min and the mixture was stirred for 30 min. The mixture was

then filtered through Celite under argon and the resulting solutions were analysed by NMR spectroscopy.

[Pd(η^3 -1,3-diphenylallyl)(3a)]BF₄ (19): Major isomer **A**: Yield: 65%; ¹H NMR (CD₂Cl₂): δ = 1.08 (s, 9H; CH₃, *t*Bu), 1.21 (s, 9H; CH₃, *t*Bu), 1.29 (s, 18H; CH₃, *t*Bu), 1.33 (s, 9H; CH₃, *t*Bu), 1.50 (s, 18H; CH₃, *t*Bu), 1.57 (s, 9H; CH₃, *t*Bu), 3.83 (m, 1H; NH), 5.15 (m, 1H; CH terminal), 5.35 (m, 1H; CH terminal), 5.81 (m, 1H; CH-N), 5.90 (m, 1H; CH-O), 6.68 (m, 1H; CH central), 6.57–7.81 ppm (m, 28H; CH=); ¹³C NMR (CD₂Cl₂): δ = 31.4–33.0 (CH₃, *t*Bu), 35.0–36.6 (C, *t*Bu), 57.2 (d, ³J_{C-P} = 17.5 Hz; CH-N), 85.1 (dd, J_{C-P} = 45.5 Hz, J_{C-P} = 7 Hz; CH terminal), 86.7 (m; CH-O), 99.6 (dd, J_{C-P} = 37.2 Hz, J_{C-P} = 4 Hz; CH terminal), 114.7 (m; CH central), 131.0–150.0 ppm (aromatic carbons); ³¹P NMR (CD₂Cl₂): δ = 129.0 (d, J_{P-P} = 165.3 Hz, 1P; P-O), 142.0 ppm (d, J_{P-P} = 165.3 Hz, 1P; P-N). Minor isomer **B**: Yield: 35%; ¹H NMR (CD₂Cl₂): δ = 1.29 (s, 9H; CH₃, *t*Bu), 1.32 (s, 9H; CH₃, *t*Bu), 1.53 (s, 9H; CH₃, *t*Bu), 1.54 (s, 9H; CH₃, *t*Bu), 1.80 (s, 9H; CH₃, *t*Bu), 1.87 (s, 9H; CH₃, *t*Bu), 1.88 (s, 9H; CH₃, *t*Bu), 1.90 (s, 9H; CH₃, *t*Bu), 4.06 (m, 1H; NH), 5.22 (m, 1H; CH terminal), 5.39 (m, 1H; CH terminal), 5.66 (m, 2H; CH-N, CH-O), 6.68 (m, 1H; CH central), 6.57–7.81 ppm (m, 28H; CH=); ¹³C NMR (CD₂Cl₂): δ = 31.4–33.0 (CH₃, *t*Bu), 35.0–36.6 (C, *t*Bu), 57.1 (d, ³J_{C-P} = 17.5 Hz; CH-N), 85.7 (dd, J_{C-P} = 42 Hz, J_{C-P} = 6 Hz; CH terminal), 86.7 (m; CH-O), 97.5 (dd, J_{C-P} = 31.1 Hz, J_{C-P} = 4 Hz; CH terminal), 114.5 (m; CH central), 131.0–150.0 ppm (aromatic carbons); ³¹P NMR (CD₂Cl₂): δ = 130.9 (d, J_{P-P} = 171.6 Hz, 1P; P-O), 140.4 ppm (d, J_{P-P} = 171.6 Hz, 1P; P-N); elemental analysis calcd (%) for C₈₅H₁₀₆BF₄NO₅P₂Pd: C 69.08, H 7.30, N 0.95; found: C 69.16, H 7.34, N 0.99.

[Pd(η^3 -1,3-diphenylallyl)(3d)]BF₄ (20): Isomer **A**: Yield: 46%; ¹H NMR (CD₂Cl₂): δ = -0.4–0.8 (m, 36H; CH₃-Si), 4.21 (m, 1H; NH), 5.25 (m, 1H; CH terminal), 5.56 (m, 2H; CH terminal, CH-N), 5.79 (m, 1H; CH-O), 6.78 (m, 1H; CH central), 6.8–8.0 ppm (m, 32H; CH=); ¹³C NMR (CD₂Cl₂): δ = 0.7–2.7 (CH₃-Si), 59.3 (m; CH-N), 84.3 (m; CH terminal), 87.0 (m; CH-O), 96.5 (m; CH terminal), 113.4 (m; CH central), 128.0–154.0 ppm (aromatic carbons); ³¹P NMR (CD₂Cl₂): δ = 133.1 (d, J_{P-P} = 150.4 Hz, 1P; P-O), 144.4 ppm (d, J_{P-P} = 150.4 Hz, 1P; P-N). Isomer **B**: Yield: 43%; ¹H NMR (CD₂Cl₂, 253 K): δ = -0.4–0.8 (m, 36H; CH₃-Si), 4.02 (m, 1H; NH), 5.04 (m, 1H; CH terminal), 5.48 (m, 1H; CH terminal), 5.71 (m, 1H; CH-N), 6.02 (m, 1H; CH-O), 6.78 (m, 1H; CH central), 6.8–8.0 ppm (m, 32H; CH=); ¹³C NMR (CD₂Cl₂, 253 K): δ = 0.7–2.7 (CH₃-Si), 59.3 (m; CH-N), 86.4 (m; CH terminal), 85.7 (m; CH-O), 96.2 (m; CH terminal), 113.4 (m; CH central), 128.0–154.0 ppm (aromatic carbons); ³¹P NMR (CD₂Cl₂, 253 K): δ = 133.1 (d, J_{P-P} = 152.5 Hz, 1P; P-O), 142.1 ppm (d, J_{P-P} = 152.5 Hz, 1P; P-N). Isomer **C**: Yield: 11%; ¹H NMR (CD₂Cl₂, 253 K): δ = -0.4–0.8 (m, 36H; CH₃-Si), 3.56 (m, 1H; NH), 4.49 (m, 1H; CH central), 4.80 (m, 1H; CH terminal), 5.43 (m, 1H; CH terminal), 5.84 (m, 2H; CH-O, CH-N), 6.8–8.0 ppm (m, 32H; CH=); ¹³C NMR (CD₂Cl₂, 253 K): δ = 0.7–2.7 (CH₃-Si), 59.3 (m; CH-N), 88.5 (m; CH terminal), 85.7 (m; CH-O), 95.8 (m; CH terminal), 112.9 (m; CH central), 128.0–154.0 ppm (aromatic carbons); ³¹P NMR (CD₂Cl₂, 253 K): δ = 122.7 (br, 1P; P-O), 129.8 ppm (br, 1P; P-N); elemental analysis calcd (%) for C₆₅H₇₄BF₄NO₅P₂PdSi₄: C 59.24, H 5.74, N 1.06; found: C 59.42, H 5.81, N 1.03.

[Pd(η^3 -1,3-diphenylallyl)(3f)]BF₄ (21): Major isomer **A**: Yield: 70%; ¹H NMR (CD₂Cl₂): δ = 0.1–0.9 (m, 36H; CH₃-Si), 4.24 (m, 1H; NH), 5.27 (m, 1H; CH terminal), 5.59 (m, 2H; CH terminal, CH-N), 5.82 (m, 1H; CH-O), 6.82 (m, 1H; CH central), 6.9–8.0 ppm (m, 40H; CH=); ¹³C NMR (CD₂Cl₂): δ = 0.9–3.0 (CH₃-Si), 60.1 (m; CH-N), 84.7 (dd, J_{C-P} = 42 Hz, J_{C-P} = 6 Hz; CH terminal), 89.0 (m; CH-O), 99.2 (dd, J_{C-P} = 36.2 Hz, J_{C-P} = 4 Hz; CH terminal), 114.9 (m; CH central), 128.0–154.0 ppm (aromatic carbons); ³¹P NMR (CD₂Cl₂): δ = 129.4 (d, J_{P-P} = 164.0 Hz, 1P; P-O), 141.8 (d, J_{P-P} = 164.0 Hz, 1P; P-N). Minor isomer **B**: Yield: 30%; ¹H NMR (CD₂Cl₂): δ = 0.1–0.9 (m, 36H; CH₃-Si), 4.18 (m, 1H; NH), 5.24 (m, 1H; CH terminal), 5.62 (m, 1H; CH terminal), 5.64 (m, 1H; CH-N), 5.82 (m, 1H; CH-O), 6.82 (m, 1H; CH central), 6.9–8.0 ppm (m, 40H; CH=); ¹³C NMR (CD₂Cl₂): δ = 0.9–3.0 (CH₃-Si), 60.4 (m; CH-N), 85.2 (dd, J_{C-P} = 40.2 Hz, J_{C-P} = 7 Hz; CH terminal), 89.1 (m; CH-O), 98.1 (m; CH terminal), 114.7 (m; CH central), 128.0–154.0 ppm (aromatic carbons); ³¹P NMR (CD₂Cl₂): δ = 130.1 (d, J_{P-P} = 159.4 Hz, 1P; P-O), 142.0 ppm (d, J_{P-P} = 159.4 Hz, 1P; P-N); elemental analysis calcd

(%) for C₈₁H₈₂BF₄NO₅P₂PdSi₄: C 64.09, H 5.51, N 0.92; found: C 63.89, H 5.42, N 0.88.

[Pd(η^3 -1,3-diphenylallyl)(6a)]BF₄ (22): Major isomer **A**: Yield: 54%; ¹H NMR (CD₂Cl₂, 253 K): δ = 0.86 (t, ³J_{H-H} = 8 Hz, 3H; CH₃), 1.29 (s, 18H; CH₃, *t*Bu), 1.31 (s, 9H; CH₃, *t*Bu), 1.32 (s, 27H; CH₃, *t*Bu), 1.44 (s, 9H; CH₃, *t*Bu), 1.50 (s, 9H; CH₃, *t*Bu), 3.18 (m, 1H; CH₂-O), 3.80 (m, 1H; CH-N), 3.94 (m, 1H; CH₂-O), 4.50 (m, 1H; NH), 4.94 (m, 1H; CH terminal), 5.15 (m, 1H; CH terminal), 6.50 (m, 1H; CH central), 6.70–7.70 ppm (m, 18H; CH=); ¹³C NMR (CD₂Cl₂, 253 K): δ = 11.5 (CH₃), 29.5 (CH₂), 31.3–32.2 (CH₃, *t*Bu), 34.5–36.2 (C, *t*Bu), 51.5 (m; CH-N), 75.0 (m; CH₂-O), 82.8 (m; CH terminal), 97.6 (m; CH terminal), 114.9 (m; CH central), 122.0–150.0 ppm (aromatic carbons); ³¹P NMR (CD₂Cl₂, 253 K): δ = 139.7 (d, J_{P-P} = 163.5 Hz, 1P; P-O), 138.5 ppm (d, J_{P-P} = 163.5 Hz, 1P; P-N). Minor isomer **B**: Yield: 40%; ¹H NMR (CD₂Cl₂, 253 K): δ = 0.74 (t, ³J_{H-H} = 7.6 Hz, 3H; CH₃), 1.17 (s, 9H; CH₃, *t*Bu), 1.25 (s, 9H; CH₃, *t*Bu), 1.33 (s, 9H; CH₃, *t*Bu), 1.42 (s, 9H; CH₃, *t*Bu), 1.43 (s, 9H; CH₃, *t*Bu), 1.47 (s, 9H; CH₃, *t*Bu), 1.49 (s, 9H; CH₃, *t*Bu), 3.42 (m, 1H; CH₂-O), 3.80 (m, 1H; CH-N), 4.04 (m, 1H; CH₂-O), 4.27 (m, 1H; NH), 4.97 (m, 1H; CH terminal), 5.09 (m, 1H; CH terminal), 6.59 (m, 1H; CH central), 6.70–7.70 ppm (m, 18H; CH=); ¹³C NMR (CD₂Cl₂, 253 K): δ = 11.0 (CH₃), 27.5 (CH₂), 31.3–32.2 (CH₃, *t*Bu), 34.5–36.2 (C, *t*Bu), 51.5 (m; CH-N), 75.0 (m; CH₂-O), 84.3 (dd, J_{C-P} = 28.2 Hz, J_{C-P} = 6 Hz; CH terminal), 95.4 (m; CH terminal), 113.0 (m; CH central), 122.0–150.0 ppm (aromatic carbons); ³¹P NMR (CD₂Cl₂, 253 K): δ = 131.4 (d, J_{P-P} = 153.8 Hz, 1P; P-O), 137.1 ppm (d, J_{P-P} = 153.8 Hz, 1P; P-N). Minor isomer **C**: Yield: 6%; ³¹P NMR (CD₂Cl₂, 253 K): δ = 139.7 (d, J_{P-P} = 163.5 Hz, 1P; P-O), 140.6 ppm (d, J_{P-P} = 163.5 Hz, 1P; P-N); elemental analysis calcd (%) for C₇₅H₁₀₂BF₄NO₅P₂Pd: C 66.54, H 7.67, N 1.03; found: C 66.87, H 7.81, N 1.00.

[Pd(η^3 -1,3-diphenylallyl)(9a)]BF₄ (23): Major isomer **A**: Yield: 60%; ¹H NMR (CD₂Cl₂, 253 K): δ = 1.15 (s, 9H; CH₃, *t*Bu), 1.24 (s, 9H; CH₃, *t*Bu), 1.27 (s, 9H; CH₃, *t*Bu), 1.28 (s, 9H; CH₃, *t*Bu), 1.46 (s, 9H; CH₃, *t*Bu), 1.47 (s, 18H; CH₃, *t*Bu), 1.53 (s, 9H; CH₃, *t*Bu), 3.20 (m, 1H; CH₂-N), 3.73 (m, 1H; CH-O), 4.66 (m, 1H; CH₂-N), 5.06 (m, 1H; CH terminal), 5.21 (m, 1H; CH terminal), 5.63 (m, 1H; H-N), 6.52 (m, 3H; CH central, CH=), 6.70–7.80 ppm (m, 21H; CH=); ¹³C NMR (CD₂Cl₂, 253 K): δ = 31.2–32.2 (CH₃, *t*Bu), 34.4–36.4 (C, *t*Bu), 46.7 (m; CH-N), 71.1 (m; CH₂-O), 84.9 (dd, J_{C-P} = 28 Hz, J_{C-P} = 6 Hz; CH terminal), 98.0 (dd, J_{C-P} = 36 Hz, J_{C-P} = 6 Hz; CH terminal), 114.5 (m; CH central), 125.0–150.0 ppm (aromatic carbons); ³¹P NMR (CD₂Cl₂, 253 K): δ = 131.2 (d, J_{P-P} = 156.9 Hz, 1P; P-O), 144.0 ppm (d, J_{P-P} = 156.9 Hz, 1P; P-N). Minor isomer **B**: Yield: 35%; ¹H NMR (CD₂Cl₂, 253 K): δ = 1.27 (s, 9H; CH₃, *t*Bu), 1.29 (s, 9H; CH₃, *t*Bu), 1.50 (s, 9H; CH₃, *t*Bu), 1.56 (s, 9H; CH₃, *t*Bu), 1.73 (s, 9H; CH₃, *t*Bu), 1.79 (s, 9H; CH₃, *t*Bu), 1.81 (s, 9H; CH₃, *t*Bu), 1.83 (s, 9H; CH₃, *t*Bu), 3.10 (m, 1H; CH₂-N), 3.81 (m, 1H; CH-O), 4.51 (m, 1H; CH₂-N), 5.10 (m, 1H; CH terminal), 5.26 (m, 1H; CH terminal), 5.45 (m, 1H; H-N), 6.52 (m, 3H; CH central, CH=), 6.70–7.80 ppm (m, 21H; CH=); ¹³C NMR (CD₂Cl₂, 253 K): δ = 31.2–32.2 (CH₃, *t*Bu), 34.4–36.4 (C, *t*Bu), 46.7 (m; CH-N), 71.1 (m; CH₂-O), 85.4 (dd, J_{C-P} = 40 Hz, J_{C-P} = 4 Hz; CH terminal), 96.4 (dd, J_{C-P} = 32 Hz, J_{C-P} = 7 Hz; CH terminal), 113.2 (m; CH central), 125.0–150.0 ppm (aromatic carbons); ³¹P NMR (CD₂Cl₂, 253 K): δ = 132.6 (d, J_{P-P} = 157.8 Hz, 1P; P-O), 143.1 ppm (d, J_{P-P} = 157.8 Hz, 1P; P-N). Minor isomer **C**: Yield: 5%; ³¹P NMR (CD₂Cl₂, 253 K): δ = 131.4 (d, J_{P-P} = 161.6 Hz, 1P; P-O), 145.2 ppm (d, J_{P-P} = 161.6 Hz, 1P; P-N); elemental analysis calcd (%) for C₇₉H₁₀₂BF₄NO₅P₂Pd: C 67.69, H 7.41, N 1.00; found: C 67.92, H 7.52, N 1.04.

Pd(η^3 -1,3-dimethylallyl)(1a)]BF₄ (24): Major isomer **A**: Yield: 65%; ¹H NMR (CD₂Cl₂): δ = 1.05–1.35 (s, 6H; CH₃), 1.35–1.75 (m, 72H; CH₃, *t*Bu), 3.78 (m, 1H; CH terminal), 4.03 (m, 1H; CH terminal), 4.35 (m, 1H; CH-O), 5.28 (m, 1H; CH central), 5.85 (m, 1H; NH), 5.95 (m, 1H; CH-N), 6.70–7.70 ppm (m, 18H; CH=); ¹³C NMR (CD₂Cl₂): δ = 16.9 (CH₃), 18.0 (CH₃), 31.1–32.5 (CH₃, *t*Bu), 34.8–36.0 (C, *t*Bu), 57.5 (m; CH-N), 86.6 (m; CH₂-O), 87.0 (dd, J = 37.2 Hz, J = 7.6 Hz; CH terminal), 93.9 (dd, J = 39.4 Hz, J = 7.6 Hz; CH terminal), 125.0 (m; CH central), 125.0–150.0 ppm (aromatic carbons); ³¹P NMR (CD₂Cl₂): δ = 129.3 (d, J_{P-P} = 125.8 Hz, 1P; P-O), 142.0 ppm (d, J_{P-P} = 125.8 Hz, 1P; P-N). Minor isomer **B**: Yield: 35%; ¹H NMR (CD₂Cl₂): δ = 1.05–1.35 (s, 6H; CH₃),

1.35–1.75 (m, 72H; CH₃, *t*Bu), 3.78 (m, 1H; CH terminal), 4.03 (m, 1H; CH terminal), 4.48 (m, 1H; CH-O), 5.28 (m, 1H; CH central), 5.85 (m, 2H; CH-N, NH), 6.70–7.70 ppm (m, 18H; CH=); ¹³C NMR (CD₂Cl₂): δ = 16.8 (CH₃), 18.2 (CH₃), 31.1–32.5 (CH₃, *t*Bu), 34.8–36.0 (C, *t*Bu), 57.3 (m; CH-N), 86.5 (m; CH₂-O), 87.0 (dd, *J* = 42.5 Hz, *J* = 5.3 Hz; CH terminal), 92.2 (dd, *J* = 35.6 Hz, *J* = 8.3 Hz; CH terminal), 124.3 (m; CH central), 125.0–150.0 ppm (aromatic carbons); ³¹P NMR (CD₂Cl₂): δ = 130.5 (d, *J*_{P,P} = 128.1 Hz, 1P; P-O), 140.4 ppm (d, *J*_{P,P} = 128.1 Hz, 1P; P-N); elemental analysis calcd (%) for C₇₅H₁₀₂BF₄NO₅P₂Pd: C 66.54, H 7.67, N 1.03; found: C 66.34, H 7.63, N 1.08.

Pd(η³-1,3-dimethylallyl)(2a)BF₄ (25): Major isomer **A**: Yield: 65%; ¹H NMR (CD₂Cl₂): δ = 1.1–1.3 (s, 9H; CH₃), 1.3–1.70 (m, 72H; CH₃, *t*Bu), 3.86 (m, 3H; 2 × CH terminal, NH), 4.88 (m, 1H; CH-O), 5.18 (m, 1H; CH central), 5.59 (m, 1H; CH-N), 7.1–7.70 ppm (m, 13H; CH=); ¹³C NMR (CD₂Cl₂): δ = 16.5 (CH₃), 18.1 (CH₃), 16.7 (CH₃), 31.0–32.3 (CH₃, *t*Bu), 34.8–36.0 (C, *t*Bu), 50.0 (m; CH-N), 86.3 (m; CH₂-O), 90.0 (m; CH terminal), 93.6 (dd, *J* = 40.2 Hz, *J* = 7.1 Hz; CH terminal), 124.6 (m; CH central), 125.0–150.0 ppm (aromatic carbons); ³¹P NMR (CD₂Cl₂): δ = 130.4 (d, *J*_{P,P} = 123.7 Hz, 1P; P-O), 139.1 ppm (d, *J*_{P,P} = 123.7 Hz, 1P; P-N). Minor isomer **B**: Yield: 35%; ¹H NMR (CD₂Cl₂): δ = 1.1–1.3 (s, 9H; CH₃), 1.3–1.70 (m, 72H; CH₃, *t*Bu), 3.86 (m, 3H; 2 × CH terminal, NH), 4.88 (m, 1H; CH-O), 5.18 (m, 1H; CH central), 5.52 (m, 1H; CH-N), 7.1–7.70 ppm (m, 13H; CH=); ¹³C NMR (CD₂Cl₂): δ = 16.8 (CH₃), 18.1 (CH₃), 16.7 (CH₃), 31.0–32.3 (CH₃, *t*Bu), 34.8–36.0 (C, *t*Bu), 50.1 (m; CH-N), 86.4 (m; CH₂-O), 87.0 (dd, *J* = 38.8 Hz, *J* = 8.6 Hz; CH terminal), 90.0 (m; CH terminal), 124.0 (m; CH central), 125.0–150.0 ppm (aromatic carbons); ³¹P NMR (CD₂Cl₂): δ = 131.2 (d, *J*_{P,P} = 125.8 Hz, 1P; P-O), 138.4 ppm (d, *J*_{P,P} = 125.8 Hz, 1P; P-N); elemental analysis calcd (%) for C₇₀H₁₀₀BF₄NO₅P₂Pd: C 65.09, H 7.88, N 1.08; found: C 65.13, H 7.89, N 1.05.

Study of the reactivity of [Pd(η³-1,3-diphenylallyl)(L)]BF₄ (L = **3a and **3d**) with sodium malonate by in situ NMR spectroscopy:**^[19] A solution of in situ prepared [Pd(η³-1,3-diphenylallyl)(L)]BF₄ (L = phosphite-phosphoramidite, 0.05 mmol) in CD₂Cl₂ (1 mL) was cooled in an NMR tube at –80 °C. At this temperature, a solution of cooled sodium malonate (0.1 mmol) was added. The reaction was then followed by ³¹P NMR spectroscopy. The relative reaction rates were calculated by using a capillary containing a solution of triphenylphosphine in CD₂Cl₂ as the external standard.

Typical procedure for the allylic alkylation of *rac*-1,3-diphenyl-3-acetoxyprop-1-ene (S1): A degassed solution of [Pd(μ-Cl)(η³-C₃H₅)₂] (0.9 mg, 0.0025 mmol) and the phosphite-phosphoramidite (0.0055 mmol) in dichloromethane (0.5 mL) was stirred for 30 min. Subsequently a solution of **S1** (126 mg, 0.5 mmol) in dichloromethane (1.5 mL), dimethyl malonate (171 μL, 1.5 mmol), *N,O*-bis(trimethylsilyl)acetamide (370 μL, 1.5 mmol) and a pinch of KOAc were added. The reaction mixture was stirred at room temperature. After the desired reaction time, the mixture was diluted with Et₂O (5 mL) and a saturated NH₄Cl(aq) solution (25 mL) was added. The mixture was extracted with Et₂O (3 × 10 mL) and the extract dried with MgSO₄. The solvent was removed and conversions were measured by ¹H NMR spectroscopy. To determine the enantiomeric excesses by HPLC (Chiracel OD, 0.5% 2-propanol/hexane, flow 0.5 mL min⁻¹), samples were filtered through basic alumina using dichloromethane as the eluent.

Typical procedure for the allylic amination of *rac*-1,3-diphenyl-3-acetoxyprop-1-ene (S1): A degassed solution of [Pd(μ-Cl)(η³-C₃H₅)₂] (0.9 mg, 0.0025 mmol) and the phosphite-phosphoramidite (0.0055 mmol) in dichloromethane (0.5 mL) was stirred for 30 min. Subsequently a solution of **S1** (126 mg, 0.5 mmol) in dichloromethane (1.5 mL) and benzylamine (131 μL, 1.5 mmol) were added. The reaction mixture was stirred at room temperature. After the desired reaction time, the mixture was diluted with Et₂O (5 mL) and a saturated NH₄Cl(aq) solution (25 mL) was added. The mixture was extracted with Et₂O (3 × 10 mL) and the extract dried with MgSO₄. The solvent was removed and conversions were measured by ¹H NMR spectroscopy. To determine the enantiomeric excesses by HPLC (Chiracel OJ, 13% 2-propanol/hexane, flow 0.5 mL min⁻¹), samples were filtered through silica using 10% Et₂O/hexane mixture as the eluent.

Typical procedure for the allylic alkylation of ethyl *rac*-(*E*)-2,5-dimethylhept-4-en-3-yl carbonate (S2): A degassed solution of [Pd(μ-Cl)(η³-C₃H₅)₂] (0.9 mg, 0.0025 mmol) and the phosphite-phosphoramidite (0.0055 mmol) in dichloromethane (0.5 mL) was stirred for 30 min. Subsequently a solution of **S2** (107.2 mg, 0.5 mmol) in dichloromethane (1.5 mL), dimethyl malonate (171 μL, 1.5 mmol), *N,O*-bis(trimethylsilyl)acetamide (370 μL, 1.5 mmol) and a pinch of KOAc were added. The reaction mixture was stirred at room temperature. After the desired reaction time, the reaction mixture was diluted with Et₂O (5 mL) and a saturated NH₄Cl(aq) solution (25 mL) was added. The mixture was extracted with Et₂O (3 × 10 mL) and the extract dried with MgSO₄. The conversions and enantiomeric excesses were determined by ¹H NMR spectroscopy using [Eu(hfc)₃] as the resolving agent.

Typical procedure for the allylic alkylation of *rac*-1,3-dimethyl-3-acetoxyprop-1-ene (S3): A degassed solution of [Pd(μ-Cl)(η³-C₃H₅)₂] (0.9 mg, 0.0025 mmol) and the phosphite-phosphoramidite (0.0055 mmol) in tetrahydrofuran (0.5 mL) was stirred for 30 min. Subsequently a solution of **S3** (64 mg, 0.5 mmol) in tetrahydrofuran (1.5 mL), dimethyl malonate (171 μL, 1.5 mmol), *N,O*-bis(trimethylsilyl)acetamide (370 μL, 1.5 mmol) and a pinch of KOAc were added. The reaction mixture was stirred at room temperature. After the desired reaction time, the reaction mixture was diluted with Et₂O (5 mL) and a saturated NH₄Cl(aq) solution (25 mL) was added. The mixture was extracted with Et₂O (3 × 10 mL) and the extract dried with MgSO₄. The conversions and enantiomeric excesses were determined by GC.

Typical procedure for the allylic alkylation of *rac*-3-acetoxycyclohexene (S4) and *rac*-3-acetoxycycloheptene (S5): A degassed solution of [Pd(μ-Cl)(η³-C₃H₅)₂] (0.9 mg, 0.0025 mmol) and the phosphite-phosphoramidite (0.0055 mmol) in tetrahydrofuran (0.5 mL) was stirred for 30 min. Subsequently a solution of substrate (0.5 mmol) in tetrahydrofuran (1.5 mL), dimethyl malonate (171 μL, 1.5 mmol), *N,O*-bis(trimethylsilyl)acetamide (370 μL, 1.5 mmol) and a pinch of KOAc were added. The reaction mixture was stirred at room temperature. After the desired reaction time, the reaction mixture was diluted with Et₂O (5 mL) and a saturated NH₄Cl(aq) solution (25 mL) was added. The mixture was extracted with Et₂O (3 × 10 mL) and the extract dried with MgSO₄. The conversions and enantiomeric excesses were determined by GC using a FS-Cyclodex β-I/P 25 m column, internal diameter 0.2 mm, film thickness 0.33 mm, carrier gas 100 kPa He, FID detector).

Typical procedure for the allylic alkylation of *rac*-1-(1-naphthyl)allyl acetate (S6) and 1-(1-naphthyl)-3-acetoxyprop-1-ene (S7): A degassed solution of [Pd(μ-Cl)(η³-C₃H₅)₂] (1.8 mg, 0.005 mmol) and the phosphite-phosphoramidite (0.011 mmol) in dichloromethane (0.5 mL) was stirred for 30 min at room temperature. Subsequently a solution of substrate (0.5 mmol) in dichloromethane (1.5 mL), dimethyl malonate (171 μL, 1.5 mmol), *N,O*-bis(trimethylsilyl)acetamide (370 μL, 1.5 mmol) and a pinch of KOAc were added. After 2 h the reaction mixture was diluted with Et₂O (5 mL) and a saturated NH₄Cl(aq) solution (25 mL) was added. The mixture was extracted with Et₂O (3 × 10 mL) and the extract dried with MgSO₄. The solvent was removed and the conversions and regioselectivities were measured by ¹H NMR spectroscopy. The enantiomeric excesses were determined by HPLC (Chiralcel OJ, 13% 2-propanol/hexane, flow 0.7 mL min⁻¹), samples were filtered through basic alumina using dichloromethane as the eluent.

Acknowledgements

We are indebted to Prof. P. W. N. M. van Leeuwen, University of Amsterdam, for his comments and suggestions in the discussion on the Pd-π-allyl intermediates. We thank the Spanish Government (Consolider Ingenio CSD2006-0003, CTQ2004-04412/BQU and for a Ramon y Cajal Fellowship for O.P.) and the Catalan Government (2005SGR007777 and Distinction for the promotion of the research to M.D.) for financial support.

- [1] For reviews, see: a) J. Tsuji, *Palladium Reagents and Catalysis, Innovations in Organic Synthesis*, Wiley, New York, **1995**; b) B. M. Trost, D. L. van Vranken, *Chem. Rev.* **1996**, *96*, 395; c) A. Pfaltz, M. Lautens in *Comprehensive Asymmetric Catalysis, Vol. 2* (Eds.: E. N. Jacobsen, A. Pfaltz, H. Yamamoto), Springer, Berlin, **1999**, Chapter 24; d) B. M. Trost, M. L. Crawley, *Chem. Rev.* **2003**, *103*, 2921.
- [2] A. M. MasdeuBultó, M. Diéguez, E. Martin, M. Gómez, *Coord. Chem. Rev.* **2003**, *242*, 159, and references therein.
- [3] a) M. Diéguez, O. Pàmies, C. Claver, *J. Org. Chem.* **2005**, *70*, 3363; b) M. Diéguez, O. Pàmies, C. Claver, *Adv. Synth. Catal.* **2005**, *347*, 1257; c) M. Diéguez, S. Jansat, M. Gomez, A. Ruiz, G. Muller, C. Claver, *Chem. Commun.* **2001**, 1132; d) O. Pàmies, G. P. F. van Strijdonck, M. Diéguez, S. Deerenberg, G. Net, A. Ruiz, C. Claver, P. C. J. Kamer, P. W. N. M. van Leeuwen, *J. Org. Chem.* **2001**, *66*, 8867.
- [4] Diphosphites have recently emerged as suitable ligands for this process offering high activities, see for instance, ref. [3].
- [5] a) G. P. F. van Strijdonck, M. D. K. Boele, P. C. J. Kamer, J. G. de Vries, P. W. N. M. van Leeuwen, *Eur. J. Inorg. Chem.* **1999**, 1073; b) E. Raluy, C. Claver, O. Pàmies, M. Diéguez, *Org. Lett.* **2007**, *9*, 49.
- [6] The preliminary results were partly reported in the communication: O. Pàmies, M. Diéguez, C. Claver, *Adv. Synth. Catal.* **2007**, *349*, 836.
- [7] To the best of our knowledge there have been only two successful applications of phosphite-phosphoramidite ligands in asymmetric catalysis, see: a) ref. [5b]; b) M. Diéguez, A. Ruiz, C. Claver, *Chem. Commun.* **2001**, 2702.
- [8] O. Pàmies, M. Diéguez, G. Net, A. Ruiz, C. Claver, *Organometallics* **2000**, *19*, 1488.
- [9] Similar behaviour was observed by using diphosphite and phosphine-phosphoramidite ligands, see, for example: a) M. Diéguez, A. Ruiz, C. Claver, *Dalton Trans.* **2003**, 2957; b) M. Diéguez, O. Pàmies, A. Ruiz, C. Claver, *New J. Chem.* **2002**, *26*, 827; c) M. Diéguez, A. Ruiz, C. Claver, *J. Org. Chem.* **2002**, *67*, 3796; d) O. Pàmies, M. Diéguez, G. Net, A. Ruiz, C. Claver, *Chem. Commun.* **2000**, 2383.
- [10] L. Gong, G. Chen, A. Mi, Y. Jiang, F. Fu, X. Cui, A. S. C. Chan, *Tetrahedron: Asymmetry* **2000**, *11*, 4297.
- [11] For some successful applications, see: a) P. Dierkes, S. Randechul, L. Barloy, A. De Cian, J. Fischer, P. C. J. Kamer, P. W. N. M. van Leeuwen, J. A. Osborn, *Angew. Chem.* **1998**, *110*, 3299; *Angew. Chem. Int. Ed.* **1998**, *37*, 3116; b) B. M. Trost, A. C. Krueger, R. C. Bunt, J. Zambrano, *J. Am. Chem. Soc.* **1996**, *118*, 6520; c) O. Pàmies, M. Diéguez, C. Claver, *J. Am. Chem. Soc.* **2005**, *127*, 3646; d) Y. Mata, M. Diéguez, O. Pàmies, C. Claver, *Adv. Synth. Catal.* **2005**, *347*, 1943.
- [12] For some successful applications, see: a) B. M. Trost, R. C. Bunt, *J. Am. Chem. Soc.* **1994**, *116*, 4089; b) B. Wiese, G. Helmchen, *Tetrahedron Lett.* **1998**, *39*, 5727; c) G. Helmchen, A. Pfaltz, *Acc. Chem. Res.* **2000**, *33*, 336.
- [13] In contrast to the palladium catalytic systems, the iridium, ruthenium and molybdenum catalysts provide very high selectivity for attack on the non-terminal carbon atom to give the chiral product. See, for instance: a) C. Bruneau, J. L. Renaud, B. Demersemen, *Chem. Eur. J.* **2006**, *12*, 5178; b) A. V. Malkov, L. Gouriou, G. C. Lloyd-Jones, I. Starý, V. Langer, P. Spoor, V. Vinader, P. Košovsky, *Chem. Eur. J.* **2006**, *12*, 6910; c) B. M. Trost, S. Hildbrand, K. Dogra, *J. Am. Chem. Soc.* **1999**, *121*, 10416; d) A. Alexakis, D. Polet, *Org. Lett.* **2004**, *6*, 3529.
- [14] For recent successful applications of palladium catalysts, see: a) S.-L. You, X.-Z. Zhu, Y.-M. Luo, X.-L. Hou, L.-X. Dai, *J. Am. Chem. Soc.* **2001**, *123*, 7471; b) R. Prétôt, A. Pfaltz, *Angew. Chem.* **1998**, *110*, 337; *Angew. Chem. Int. Ed.* **1998**, *37*, 323; c) R. Hilgraf, A. Pfaltz, *Synlett* **1999**, 1814.
- [15] S. Deerenberg, H. S. Schrekker, G. P. F. van Strijdonck, P. C. J. Kamer, P. W. N. M. van Leeuwen, J. Fraanje, K. Goubitz, *J. Org. Chem.* **2000**, *65*, 4810.
- [16] A. Gogoll, J. Örnebro, H. Grennberg, J. E. Bäckvall, *J. Am. Chem. Soc.* **1994**, *116*, 3631.
- [17] This is in agreement with the fact that the exchange rate constant between isomers **A** and **B** is faster than the catalytic rate constants of isomers **A** and **B**.
- [18] G. J. H. Buisman, P. C. J. Kamer, P. W. N. M. van Leeuwen, *Tetrahedron: Asymmetry* **1993**, *4*, 1625.
- [19] R. J. van Haaren, P. H. Keeven, L. A. van der Veen, K. Goubitz, G. P. F. van Strijdonck, H. Oevering, J. N. H. Reek, P. C. J. Kamer, P. W. N. M. van Leeuwen, *Inorg. Chim. Acta* **2002**, *327*, 108.

Received: June 4, 2007

Published online: November 2, 2007